12-1-2011

Diffusion tensor imaging data reveals GRM3 polymorphism's association with white matter integrity in schizophrenia

Joanna Mounce

Joanna Mounce

Candidate

Biomedical Sciences (Neurosciences)

Department

This thesis is approved, and it is acceptable in quality and form for publication:

Approved by the Thesis Committee:

Dr. Nora Perrone-Bizzozero, Chairperson

Dr. Vince Calhoun

Dr. Christine Stidley

Dr. Jessica Turner

DIFFUSION TENSOR IMAGING DATA REVEALS GRM3 POLYMORPHISM'S ASSOCIATION WITH WHITE MATTER INTEGRITY IN SCHIZOPHRENIA

by

Joanna Mounce
B.S. Biology, New Mexico State University, 2008

THESIS

Submitted in Partial Fulfillment of the
Requirements of the Degree of

Master of Science in Biomedical Sciences

The University of New Mexico
Albuquerque, New Mexico

December, 2011

DIFFUSION TENSOR IMAGING DATA REVEALS GRM3 POLYMORPHISM'S ASSOCIATION WITH WHITE MATTER INTEGRITY IN SCHIZOPHRENIA

By
Joanna Mounce

B.S. Biology, New Mexico State University, 2008
M.S., Biomedical Sciences, University of New Mexico, 2011

ABSTRACT

While the functional disconnectivity hypothesis of schizophrenia has been the subject of much study, very little is known about the contribution of individual genotypes to connectivity between brain regions in either schizophrenia patients or in healthy controls.

In this study, we obtained diffusion tensor imaging (DTI) maps and genome-wide SNP data from 74 cases and 87 age- and gender-matched controls. Correlations were performed between loading coefficients obtained from fractional anisotropy (FA) values in networks of regions representing 6 maximally independent components and 134 SNPs in genes that have been found to be important in myelination and/or schizophrenia. By using independent component analysis (ICA) to analyze the FA data we move beyond single voxels (voxel based morphometry) to a source based morphometry. In doing so, we can obtain networks of FA values that covary in a similar way among subjects, and we can study the relationship between these networks and genotype. We report one SNP located in the intronic region of the metabotropic glutamate receptor 3 gene *GRM3* that showed a significant correlation with connectivity in patients but not in controls ($p<1.0x10^{-4}$). This SNP, rs7808623, has not been previously shown to be associated with schizophrenia, although association has been shown with several SNPs in *GRM3*.

Table of Contents

LIST OF FIGURES

LIST OF TABLES

CHAPTER 1: INTRODUCTION

Schizophrenia is a debilitating psychiatric disease that affects approximately 1% of the population across the world. Psychiatrists characterize schizophrenia by the presence of both positive and negative symptoms. Positive symptoms include hallucinations and delusions, whereas negative symptoms include flat affect and asociality. Schizophrenia heritability is thought to be approximately 50% based on twin studies, with an apparently complex interplay occurring between genes and environment (Brown, 2011; O'Connell et al., 2011). Because many of the risk factors for schizophrenia occur during prenatal life, schizophrenia is widely thought to be a developmental disorder. Adding strength to this hypothesis is the fact that the age of onset for schizophrenia is usually in late adolescence.

The functional disconnectivity hypothesis of schizophrenia states that symptoms of schizophrenia can at least in part be explained by a loss of connectivity between dispersed brain regions. Studies investigating this hypothesis usually focus on myelin integrity and oligodendrocyte development which are necessary for proper signaling of the many myelinated tracts in the central nervous system. This hypothesis is attractive because myelination of some tracts in the limbic system occurs in late adolescence, which is the same time as the usual age of onset for schizophrenia (Benes, 1989). In addition, both schizophrenia and myelination have been found to be affected by an interplay between genes and the environment, with adverse environmental conditions decreasing myelination and increasing risk for developing schizophrenia (Brouwer et al., 2010). The functional disconnectivity hypothesis has been experimentally supported by several post-mortem microarray analyses that have identified several genes in myelin and

oligodendrocyte related pathways that are differentially expressed in the brains of schizophrenia patients (e.g. Aston et al., 2004; Barley et al., 2009; Hakak et al., 2001; Haroutunian et al., 2007). In most instances, myelin and oligodendrocyte genes have been found to be expressed at a lower level in schizophrenia patients compared to controls. In addition, pure demyelinating disorders, such as metachromatic leukodystrophy, can result in psychosis when the age of onset occurs in late adolescence (Walterfang et al., 2005).

While most support for the functional disconnectivity hypothesis has come from post-mortem studies, there have been several studies showing specific SNPs in myelin related genes that are over-represented in people with schizophrenia compared to controls (e.g. Buxbaum et al., 2008; Qu et al, 2008). For this study, we investigated the presence of 134 SNPs from genes that have been previously shown to be involved in myelin and oligodendrocyte function (Jungerius et al., 2008), as well as from genes that have been shown to be associated with schizophrenia in general (http://www.szgene.org, see Appendix A for a list of all SNPs).

Diffusion tensor imaging (DTI) is an application of magnetic resonance imaging that uses magnetic gradients to infer information about water diffusion in living tissue (Basser et al., 1994). In most tissues, including grey matter and ventricles in the brain, water shows random, isotropic diffusion. However, fibrous tissues like myelinated axonal tracts in the brain only allow water to diffuse along the axon of the fiber in an anisotropic fashion. A measure of anisotropy of diffusion, called fractional anisotropy (FA), can be used as a measure of the functional connectivity in each voxel of the DTI image. Functional connectivity and FA change depending on axon myelination, axon diameter, axon density, and/or directional coherence of axons (Basser, 1995). Although more than

one factor can affect FA, it has generally been used in the literature as a marker of white matter integrity and myelination. In agreement with post-mortem gene expression studies, most studies have reported that patients with schizophrenia have lower FA values in at least one white matter tract. In particular, the interhemispheric fibers, anterior thalamic radiation (ATR), inferior longitudinal fasciculi, inferior frontal occipital fasciculi, cingulum and fornix have all been implicated in schizophrenia by a recent meta-analysis (Bora et al., 2011).

Following image acquisition, we used independent component analysis (ICA) to process DTI data into maximally independent components (Arfanakis, 2002). ICA is a blind source separation technique that is widely used in fMRI studies. Although ICA has not been widely used in DTI studies, it may offer several advantages over traditional tract –based data analysis techniques (Li et al., 2011). Firstly, as a data-driven technique, ICA does not automatically treat FA values across whole tracts as constant averages. Secondly, ICA does not assume independence of individual whole-tracts, an assumption that both Wahl et al. (2010) and Li et al. (2011) showed to be untrue. Thirdly, as a hypothesis free technique, ICA reduces dimensionality in a logical way without discarding information across the brain. Finally, it has been suggested that ICA may be more appropriate to discover group differences between patient and control groups because individual components are determined by the variation of white matter across subjects (Li et al., 2011). However, while our ICA results yielded 6 anatomically and functionally relevant components, interpretation of these components requires care as it is not as straightforward as tract based techniques.

After obtaining biologically relevant independent components, we performed multiple correlations of component loading coefficients with the genotypes of patients and controls at 134 different SNP loci to ascertain any relationship between genotype and white matter integrity (Figure 1). Because myelin integrity has been shown to be decreased in patients with schizophrenia, we hypothesized that the genotypes of individual SNPs in genes associated with white matter integrity or schizophrenia would correlate with FA more strongly in our patient sample. We report one SNP, rs7808623, which correlates significantly (corrected $p<0.05$) with white matter integrity in our patient sample only. This correlation occurred in a component that contains a large portion of the cortico-cerebellar-thalamic-cortical circuit, a circuit which has been proposed to account for many of the diverse symptoms in schizophrenia (Andreasen et al., 1998). Rs7808623 is located in an intronic region of *GRM3*, the gene encoding metabotropic glutamate receptor 3. While polymorphisms in *GRM3* have been shown to be associated with schizophrenia (Cherlyn et al., 2010), any relationship between *GRM3* genotype and myelination has not yet been investigated. This study supports others that have shown a relationship between the glutamatergic system and white matter development and function (Matute 2011; Wake et al., 2011) and is the first to investigate the relationship between schizophrenia, functional connectivity, and genotype in many of the original 134 SNPs.

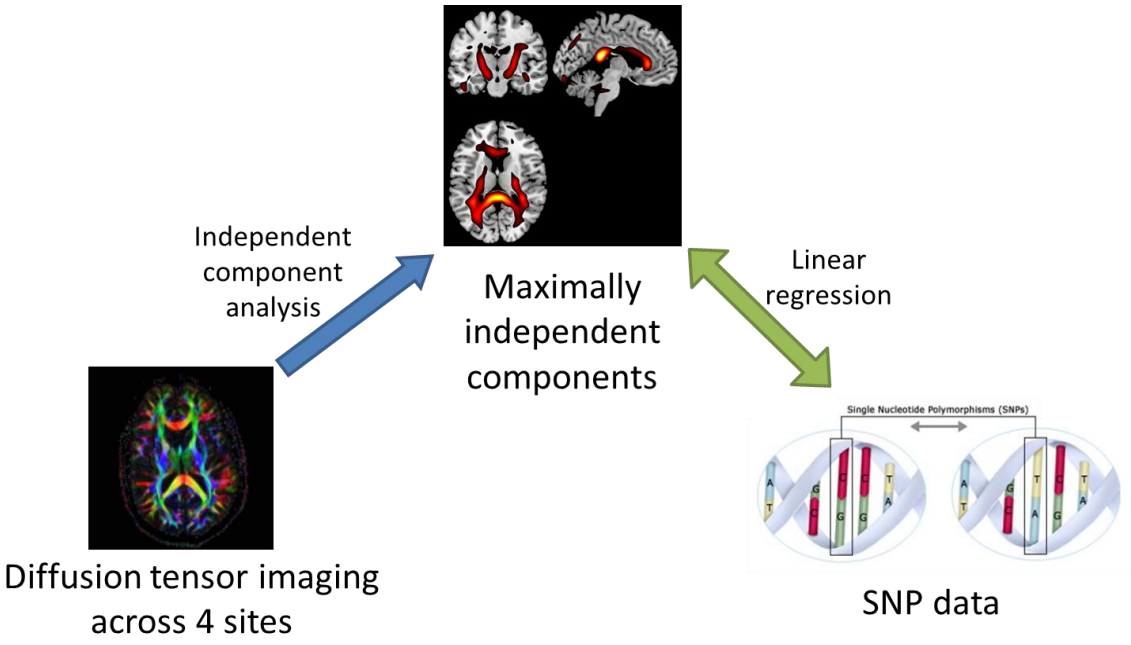

Figure 1: Experimental design
Diffusion tensor images were obtained for a sample of schizophrenia patients and controls from 4 different sites. ICA was then performed to obtain 20 independent components, six of which were determined to be biologically meaningful. The loading coefficients of these components for each subject were then analyzed for case/control differences, medication effects, symptom severity effects, and associations with genotype in 134 myelin and schizophrenia related SNPs.

CHAPTER 2: METHODS

Sample

The subjects for this study were participants in the Mind Clinical Imaging Consortium (MCIC), a multi-site study involving investigators from New Mexico (UNM), Iowa (IA), Massachusetts General Hospital (MGH), and Minnesota (MINN) (Abbott et al., 2011). The cross section of individuals from the MCIC study with both genetic and DTI data consisted of 75 cases and 87 controls matched for age and sex. Unfortunately, these groups were not matched for race, and white/non-white status was included as a covariate for all linear regression analyses that compared cases and controls with no change in results. One case subject had to be excluded because of poor DTI image quality, leaving a final sample of 74 subjects and 87 controls (Table 1).

	Schizophrenia (n=74)	Controls (n=87)	P value (test)
Age			
Mean (SD)	34.8 (11.1)	32.7 (11.2)	0.41 (Two sample Kolmogorov-Smirnov test)
Range	18-60	18-57	
Sex (M/F)	53/21	52/35	0.16 (X^2 test)
Race/Ethnicity			
White	50	77	8.1×10^{-4} (Fisher's exact test)
Black	15	3	
Asian	4	3	
Native American	1	0	
Unknown	4	4	

Table 1: Demographic information for subjects used in this study. All subjects were members of the Mind Clinical Imaging Consortium (MCIC)

All participants provided written informed consent, and the institutional review board at each of the four sites approved this project. Participants in the control group were negative for any medical, neurological, or psychiatric illnesses. All participants in the patient group had received a diagnosis of schizophrenia, schizoaffective disorder, or

schizophreniform disorder. This diagnosis was confirmed upon their entry into the study using the Structured Clinical Interview for DSM-IV-TR Disorders (First et. al., 1997) or the Comprehensive Assessment of Symptoms and History (Andreasen et al, 1992). Patients were excluded if they had ever been diagnosed with any other psychiatric disease or with epilepsy, had a history of head injury, had a history of inhalant use, showed substance abuse or dependence within the past month, or had an intelligence quotient equal to or less than 70.

Diffusion tensor imaging data acquisition and processing

Diffusion tensor imaging data was acquired at each of four sites: UNM, IA, MGH and MINN. All sites except UNM used a Siemens 3 Tesla Trio Scanner. UNM used a 1.5 Tesla Sonata. All sites used a field of view of 256mmx256mm. UNM and MINN used 12 gradient directions with b=1000 s/mm^2, whereas IA used 6 gradient directions with b=1000 s/mm^2, and MGH used 60 gradient directions with b=700 s/mm^2. All sites imaged 64 slices, except MGH which imaged 60 slices. DTI experiments were repeated twice to increase signal-to-noise ratio.

The dicom2nii program found at www.sph.sc.edu/comd/rorden/dicom.html was used to convert dicom files to nifti format. Dicom2nii also outputs gradient direction tables after image slice orientation correction and a b-value table. Both DTI experiments were combined into one 4D nifti file with a concatenated table of corresponding b-value and gradient direction tables. Correction for Eddy currents was performed by registering all the images to a b=0 s/mm^2 diffusion image using FLIRT (FSL,

www.fmrib.ox.ac.uk/fsl) with a mutual-information cost function. This algorithm registers images of both the DTI measurements to a common image.

The diffusion tensor, scalar diffusion parameters (including FA) were calculated using DTIFIT (FSL). The data was not averaged for this calculation. FNIRT (FSL), a non-linear registration algorithm, was used to normalize the FA image of each subject to a 1x1x1mm^3 FA template (FMRIB58_FA_1mm) in the Montreal Neurological Institute (MNI) space. This normalized data was then down-sampled to a 2mmx2mmx2mm resolution and smoothed with a Gaussian kernel of 88 mm full width half maximum prior to independent component analysis performance.

Independent component analysis

ICA analysis is a blind source separation technique that is widely used in imaging studies, especially in fMRI. Briefly, ICA attempts to break data into maximally independent components in order to ascertain sources within very large data sets. ICA was performed in Matlab using Group ICA fMRI Toolbox (GIFT) software (http://icatb.sourceforge.net) to extract 20 independent components from a subject-by-voxel FA matrix (Calhoun et al., 2001; Erhardt, et al., 2010; Li, et al. 2007; Xu, et al. 2009). We chose to set the number of components at 20 based on previous observations by our lab group that this number works well with imaging data and returns biologically meaningful components. Components were visualized using MRIcron, a visualization tool freely available online at http://www.cabiatl.com/mricro/mricron/index.html.

White matter characterization of biologically relevant independent components

The white matter tracts in each component were determined in three different ways. Quantitatively, SPM8 was used to map each component to the John Hopkins DTI atlas (Mori, et al., 2005). This allowed us to view the percent of 20 different tracts in each component, as well as the percent of each component which was composed of each of the 20 different tracts (see Table 2 for white matter tracts). Qualitatively, we also used Mori et al.'s 2005 MRI Atlas of Human White Matter and http://www.dtiatlas.org (based on Wakana et al., 2004) to map the regions in component B's threshold map (Figures 2 and 9) to previously defined white matter tracts. This map represents the voxels that contribute the most to the make-up of component B. The threshold was determined by viewing which score was able to best eliminate artifacts while maintaining information about white matter tracts across all slices of all six biologically relevant maps. The qualitative analysis has the advantage of allowing us to visualize more than just the 20 white matter tracts from the SPM analysis, as well as to see the extent of connectivity between these tracts.

Determination of symptom severity and white matter association in patient sample

The severity of positive and negative symptoms for the patient group was assessed using the Scale for the Assessment of Positive Symptoms (SAPS) (Andreasen, 1984) and the Scale for the Assessment of Negative Symptoms (SANS) (Andreasen, 1983). Linear regressions were performed in R by modeling subjects' ICA loading coefficients as a function of positive, negative, or disorganized symptom scores, with site set up as a series of indicator variables.

Name of tract	Abbreviation for tract
Anterior thalamic radiation left	Left ATR
Anterior thalamic radiation right	Right ATR
Corticospinal tract left	Left CST
Corticospinal tract right	Right CST
Cingulum (cingulate gyrus) left	Left CGC
Cingulum (cingulate gyrus) right	Right CGC
Cingulum (hippocampus) left	Left CGH
Cingulum (hippocampus) right	Right CGH
Forceps major	FMAJ
Forceps minor	FMIN
Inferior fronto-occipital fasciculus left	Left IFO
Inferior fronto-occipital fasciculus right	Right IFO
Inferior longitudinal fasciculus left	Left ILF
Inferior longitudinal fasciculus right	Right ILF
Superior longitudinal fasciculus left	Left SLF
Superior longitudinal fasciculus right	Right SLF
Uncinate fasciculus left	Left UF
Uncinate fasciculus right	Right UF
Superior longitudinal fasciculus (temporal part) left	Left SLFt
Superior longitudinal fasciculus (temporal part) right	Right SLFt

Table 2: List of 20 tracts that were mapped to each of the biologically relevant components using SPM. Atlas used for map was taken from John Hopkin's DTI atlas (Mori et al., 2005)

Calculation of CPZ dose-year equivalent values in patient sample and regression with ICA loading coefficients

Medication information was also obtained for each patient and converted to lifetime CPZ equivalence values based on the expert consensus guideline presented by Kane et al., 2003. Dose year of antipsychotics were calculated using the formula described by Abbott et al., 2011:

Dose year=[(dose(mg)*100CPZ)/drugequivalent]*[daysondose/365.25]*[1year/(100CPZ*1year)]

Following calculation of dose year equivalents, linear regression was once again performed in R modeling ICA loading coefficient as a function of CPZ dose-year equivalents with site as a covariate.

Statistical analysis of components prior to integration of genotype data

After components were determined, any differences based on site were assessed using a one way ANOVA. Differences in components between cases and controls were assessed using the following linear regression model:

$$Y= \alpha + \beta_1 X_1 + \beta_2 X_2 + \beta_3 X_3 + \beta_4 X_4 + \beta_5 X_5$$

Where Y is the subjects' ICA loading coefficient values for each component, α is the intercept, X_1 is disease state, and X_2-X_4 are a series of indicator variables representing the four different sites, and X_5 is white/non-white status for each patient. P-values were adjusted using a Bonferroni correction for 6 independent tests.

Effects of medication analysis and symptom severity on ICA loading coefficient values in the patient sample were assessed using the following linear regression analyses:

$$Y= \alpha + \beta_1 X_1 + \beta_2 X_2 + \beta_3 X_3 + \beta_4 X_4$$

Where Y is the subjects' ICA loading coefficient value for each component, α is the intercept, X_1 is either lifetime medication use or symptom severity, and X_2-X_4 are a series of indicator variables representing the four different sites. P-values were adjusted using a Bonferroni correction for 6 independent tests.

Genetic analysis

All subjects were genotyped using an Illumina's HumanOmni Quad Duo Chip. A list of 288 myelin and/or schizophrenia related SNPs for further analysis was compiled

using http://www.szgene.org, Jungerius et al. (2008) and various other literature sources. Out of these 288, 140 were available from the Illumina Chip, although one failed quality control (genotyping rate<95%), and five others were excluded because they had a minor allele frequency of less than 5% in our sample. This left a final list of 134 myelin and/or schizophrenia-related SNPs (Appendix A). Allele frequency differences between cases and controls was determined using a X^2 analysis, and no genotype was present at differing rates in either sample (uncorrected p>.001). Linkage disequilibrium units for Table 3 were determined using the HapMap project's data within Applied Biosystems SNPbrowser software (http://marketing.appliedbiosystems.com/mk/get/snpb_landing).

Linear regression analyses of genotype

Genotypes were either represented as number of major alleles (i.e., 0, 1 or 2 for each SNP in each subject), or they were coded by presence of a minor allele (i.e., either 1 or 2). Pearson correlation coefficients and significance were then determined for each SNP-component combination using R. Because of the need to correct for site, linear regression was also performed modeling ICA loading coefficient value as a function of genotype and site by fitting the following model:

$$Y= \alpha + \beta_1 X_1 + \beta_2 X_2 + \beta_3 X_3 + \beta_4 X_4$$

Where Y is the subjects' ICA loading coefficient values for each component, α is the intercept, X_1 is the number of major alleles for each genotype, and X_2-X_4 are a series of indicator variables representing the four different sites. This type of test assumes an additive model for major allele presence, although similar results were obtained when a one-way ANOVA was performed for each SNP/component combination (without

correcting for site). P values for coefficients of interest were adjusted using a Bonferroni correction for 804 independent tests (134 SNPs * 6 components).

Additionally, ICA loading coefficient values were also modeled as a function of genotype, medication level and site, as well as a function of genotype, age, sex, handedness, race and site.

CHAPTER 3: RESULTS

Independent Component Analysis

Out of the 20 independent components obtained, six were qualitatively determined to be biologically meaningful (Figure 2 A-F). These components will hereafter be referred to as components A-F corresponding with the order of their appearance in Figure 2. The remaining 14 were excluded from further analysis on the basis of having large portions of brain regions which appeared to be artifacts of different brain/ventricle size among participants (Figure 2G). Having such a large number of excluded components helps to assure that most of the noise caused by variation in size along the edge of the brain is excluded from our actual analysis. Additionally, the edge of the brain does not contain any large myelinated white matter tracts, so we could exclude these components without fear of losing meaningful data.

We used SPM8 to quantitatively map the biologically meaningful components to 20 tracts defined in Johns Hopkins's DTI atlas (Table 2, Mori et al., 2005). This allowed us to view both the percentage of each tract in each component (Figure 3) as well as the percentage of each component occupied by each tract (Figure 4). Tracts which are especially represented in the biologically relevant components include the anterior thalamic radiation (ATR), the corticospinal tract (CST), the forceps major (FMAJ), forceps minor (FMIN), and the superior longitudinal fasiculus (SLF). Also, as can be seen in Figures 2-4, left-right symmetry was largely maintained in each component. This symmetry would be expected given that the same tracts on opposite sides of the brain should covary with each other.

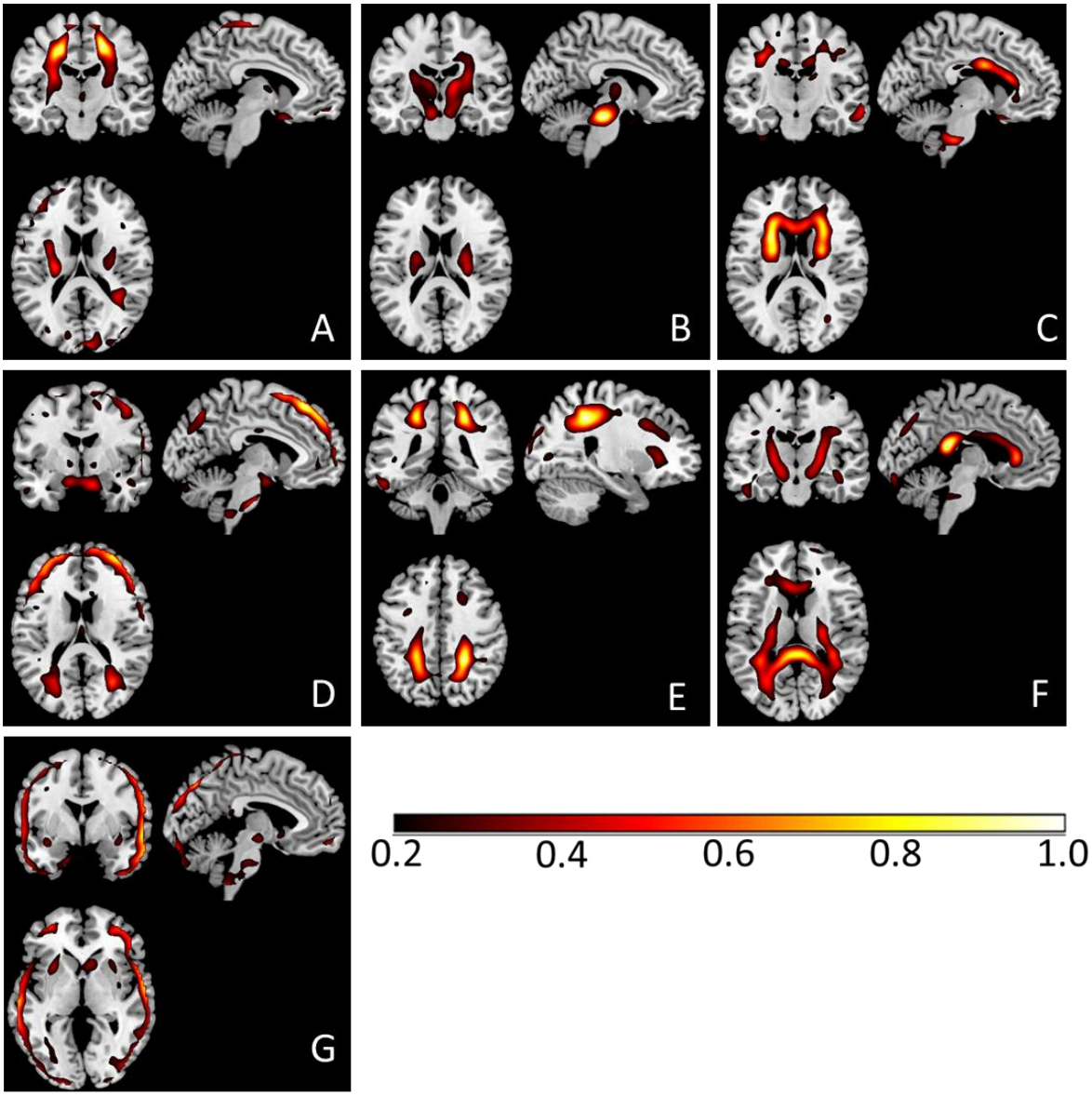

Figure 2: Threshold map for all biologically meaningful components that were observed as a result of ICA on multi-site DTI data (A-F) as well as an example of a non-biologically meaningful component (G). Color represents the extent that each voxel contributes to the map of each component. The higher contributing voxels from each biologically relevant component tend to be distributed symmetrically and along regions of white matter tracts. The voxels above threshold in the non-biologically relevant components tended to be present along the edge of the brain and may represent variation in brain size or in grey matter structure.

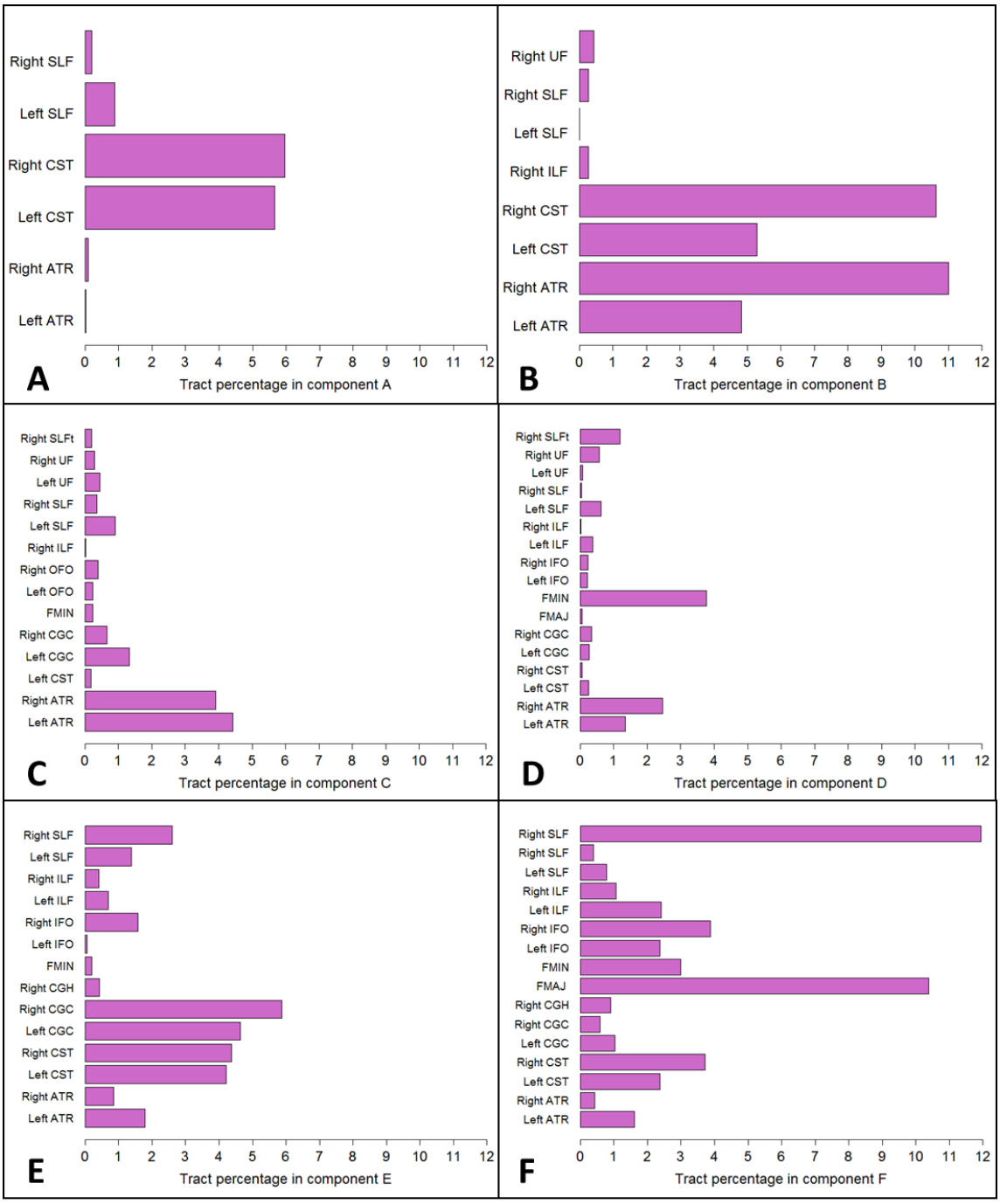

Figure 3: SPM was used to map each component to a DTI atlas containing 20 different tracts (table 2). For components A-F the percentage of each tract that is present in each component is shown.

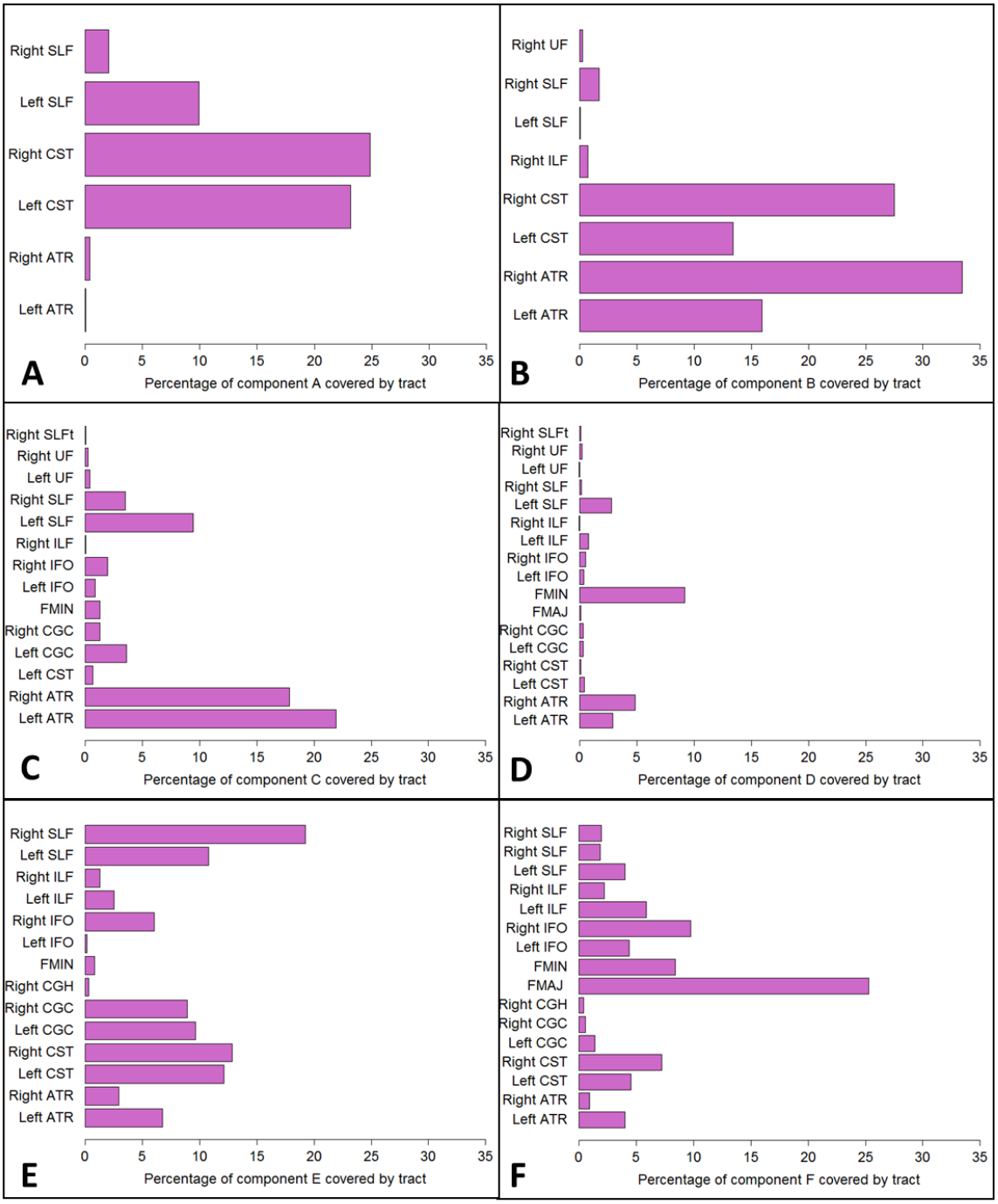

Figure 4: SPM was used to map each component to a DTI atlas containing 20 different tracts (table 2). For components A-F the percentage of each component that is covered by each tract is shown.

Site differences

We assessed the differences in DTI data between sites using a one-way ANOVA for both cases and controls in each component (Figure 5). We found that the means of ICA loading coefficients for the controls differed significantly ($p<0.05$) in each site, and that the means of the ICA loading coefficients in the schizophrenia patients differed significantly for four out of the six sites ($p>0.1$ for components B and C). In addition, using the non-parametric Fligner-Killeen test of homogeneity of variances, we found that the variances at components A, B, D, and F differed significantly both in the patient and the control group. Because of these differences, all tests subsequently performed included a correction for site. Because our results did not appear to change whether site was treated as a fixed or a random effect, we treated site as a fixed effect for ease of interpretation of our regression coefficients of interest (Bates, 2006).

Using a X^2 analysis we assessed for any differences in allele frequencies between sites. Twelve SNPs were determined to differ significantly (unadjusted $p>0.05$) by site, none of which played a role in our results. These SNPs are marked with an asterisk in Appendix A.

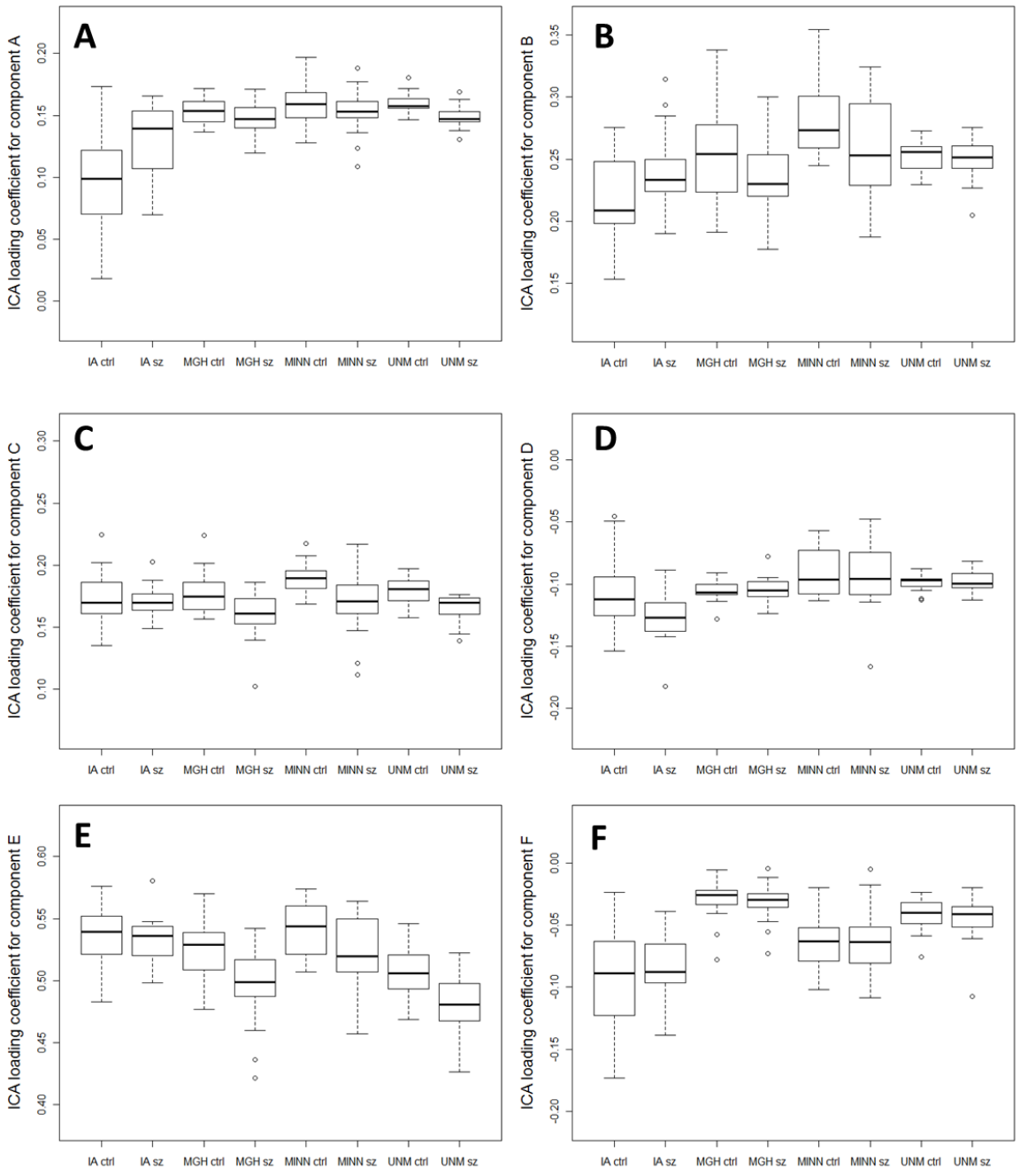

Figure 5: Box and whisker plots of the ICA loading coefficients for controls and cases at each site. The variances among control subjects and among patient subjects at site differed significantly from each other in every component except components C and E. The means of the ICA loading coefficients for the control samples at each site differed significantly from each other in each component, and the means for the patient sample differed from each other in all components except components B and C.

Differences in ICA loading coefficients in patients versus controls

ICA loading coefficients in both components C and E were determined to significantly differ between the patient group and the control group following a Bonferroni correction for 6 independent tests (Figure 6, $p=5.16x10^{-5}$ for component C and $p=3.68x10^{-5}$ for component E). As shown in Figures 3 and 4, component C contains a disproportionate portion of the ATR, while component E contains a wide variety of white matter tracts, including the ATR, the CST, the CGC, the SLF, and the right IFO. Given that component E contains a large number of tracts, the significant difference seen between white matter integrity in this component between patients and controls may be reflective of a difference in global white matter integrity.

Effects of medication on ICA loading coefficient value in patient sample

We were able to collect information on lifetime medication use in 72 out of our 74 patient subjects and convert that information into lifetime CPZ-equivalent use in dose years (Kane et al., 2003; Abbott et al., 2011). Because one subject had a lifetime CPZ-equivalent dose-year value that was more than 6 standard deviations above the mean, we excluded that subject from our analysis.

We found that lifetime medication use was significantly associated with ICA loading coefficients following a Bonferroni correction for 6 multiple comparisons in components A and E (Figure 7, corrected p=0.0131for component A and 0.00599 for component E). Interestingly, component E had also been found to differ between patients and controls, indicating that the white matter in this component may be a target of medication. As shown in Figures 3 and 4, component E contains a wide variety of white matter tracts, whereas the CST comprises a large portion of component A.

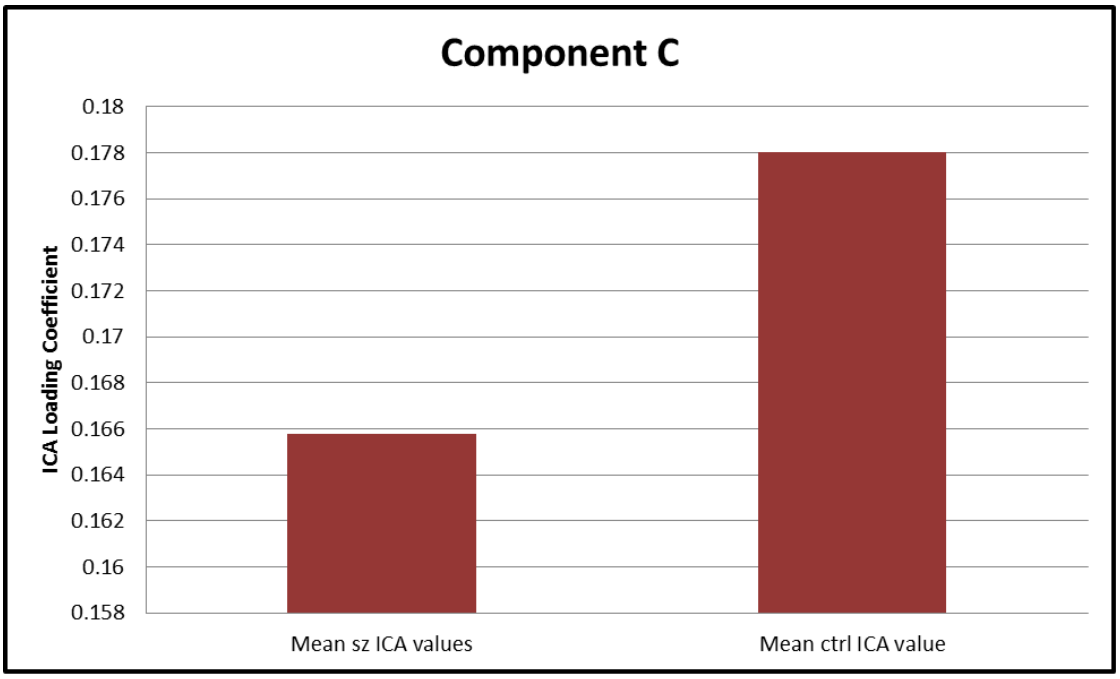

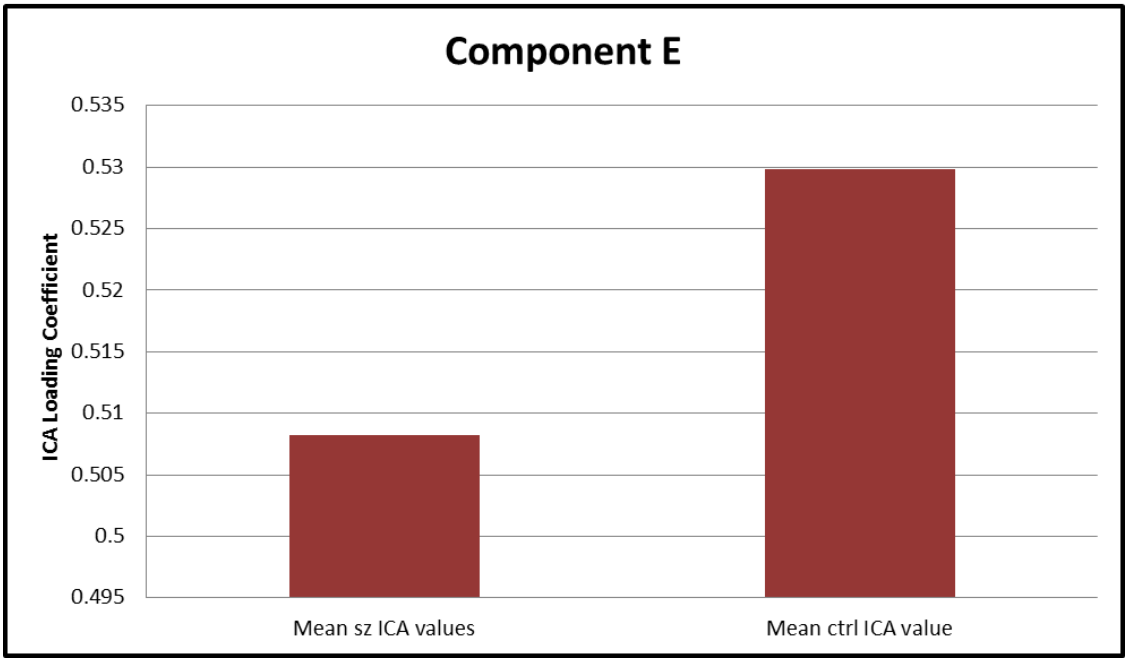

Figure 6: Mean ICA loading coefficients in both components C and F differed significantly between patients and controls when controlling for site (corrected $p=5.16 \times 10^{-5}$ for component C; corrected $p=3.68 \times 10^{-5}$ for component E).

Because 200 mg-years represented a natural break in our data (i.e., only three patients reported medication levels above 200 mg-years), we ran the same linear regression model but excluded patients whose lifetime CPZ equivalency dose-years were higher than 200 to observe whether these three subjects were driving our findings. We found that in component E medication levels were still associated with ICA loading coefficient values at a threshold-significance level (Figure 7D, uncorrected p =0.0156, corrected p=0.0936). A significant association between medication level and ICA loading coefficient was no longer seen in component A (Figure 7B, corrected p=0.451).

Effects of symptom severity scores on ICA loading coefficient values in patient sample

For our patient sample we had access to both the SAPS and SANS ratings of positive, disorganized, and negative symptom severity (Andreasen, 1983; Andreasen, 1984). We performed three linear regression analyses to assess any association between ICA loading coefficient values and symptom severity scores. These models were similar to the ones used to ascertain case/control differences and medication effects, but with X_1 representing positive, negative or disorganized symptom severity score. Surprisingly, we did not find any association between ICA loading coefficient values or symptom severity scores in any of the six biologically relevant components.

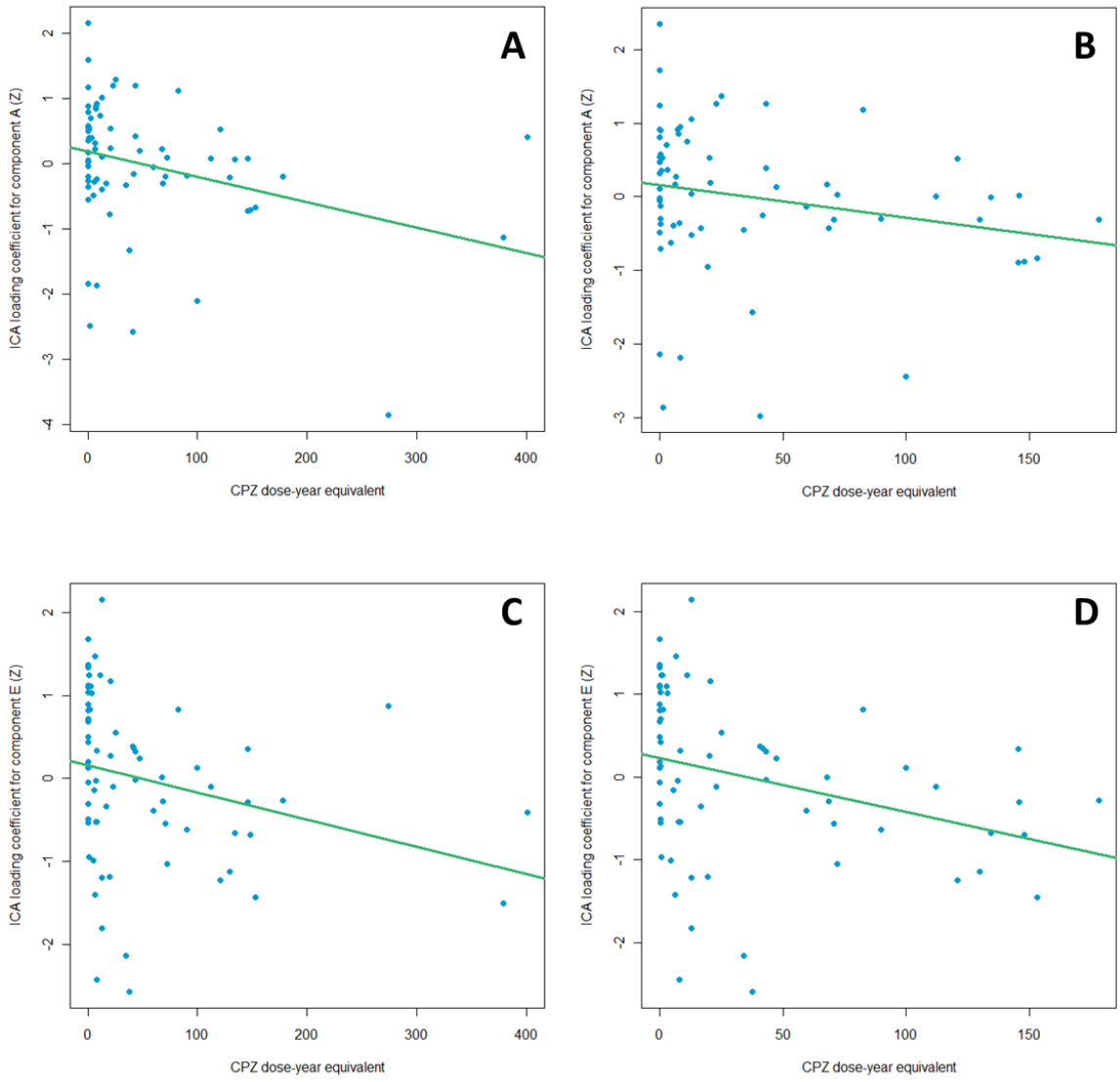

Figure 7: ICA loading coefficients for patient subjects in components A (A, B) and E (C, D) plotted as a function of lifetime CPZ dose-year equivalent use. These components showed a significant association with lifetime CPZ use when including site as a covariate (A, component A corrected p=0.0131; C, component E corrected p =0.00599) . This association was no longer significant in component A when only including patients with a lifetime CPZ equivalent of less than 200 mg-year (B, corrected p with site as a covariate=0.451), but was still significant at a threshold level for component E (D, corrected p=0.0936, uncorrected p=0.0156)

Effect of genotype on white matter integrity

After characterizing the independent components and their association with disease state, medication level, and symptom severity, we next sought to establish whether any of the six components showed an association with the genotypes of 134 myelin and schizophrenia related SNPs (Appendix A) in either the patient group or the control group.

While there were no significant effects of genotype on FA found in the control group, we report one highly significant association in the patient sample. The relationship between rs7808623, located in an intronic region of *GRM3*, and component B was found to be significant even after the stringent Bonferroni correction for 804 independent tests (corrected p=0.0252, uncorrected $p=3.14x10^{-5}$). The minor allele of rs7808623 was associated with higher white matter integrity in component B (Figure 8A), which contains portions of the ATR as well as the corticospinal tract (Figure 3B and Figure 4B). The allele frequency for rs7808623 did not differ by site (X^2 test, p=0.211). By mapping the top-contributing voxels in component B slice by slice (Figure 9) and comparing these slices with two different white matter atlases, we could see that component B represents a series of tracts connecting the frontal cortex to the cerebellum and that these tracts correspond to the cortico-cerebellar-thalamic-cortical circuit that has been implicated in schizophrenia pathology (Andreasen and Pierson, 2008).

Because there was only one patient with a homozygous minor genotype (Figure 8A), we also performed a regression analysis wherein we grouped the homozygous minor case with the heterozygous cases (Figure 8B). This design no longer represents an additive model, but looks at the difference in mean ICA loading coefficient between

subjects with or without at least one minor allele. We found that with this model the association between rs7808623 and component B was still quite significant (uncorrected $p=6.75x10^{-5}$), although it no longer passed a Bonferroni correction at the $p<0.05$ level (corrected p=0.0542). This association also remained significant when medication levels were used as an additional covariate (corrected p=0.0469). Finally, this association remained significant when using the demographic factors age, sex, handedness, and race ('non-hispanic white/other' due to sample size) as covariates (corrected p=0.0249).

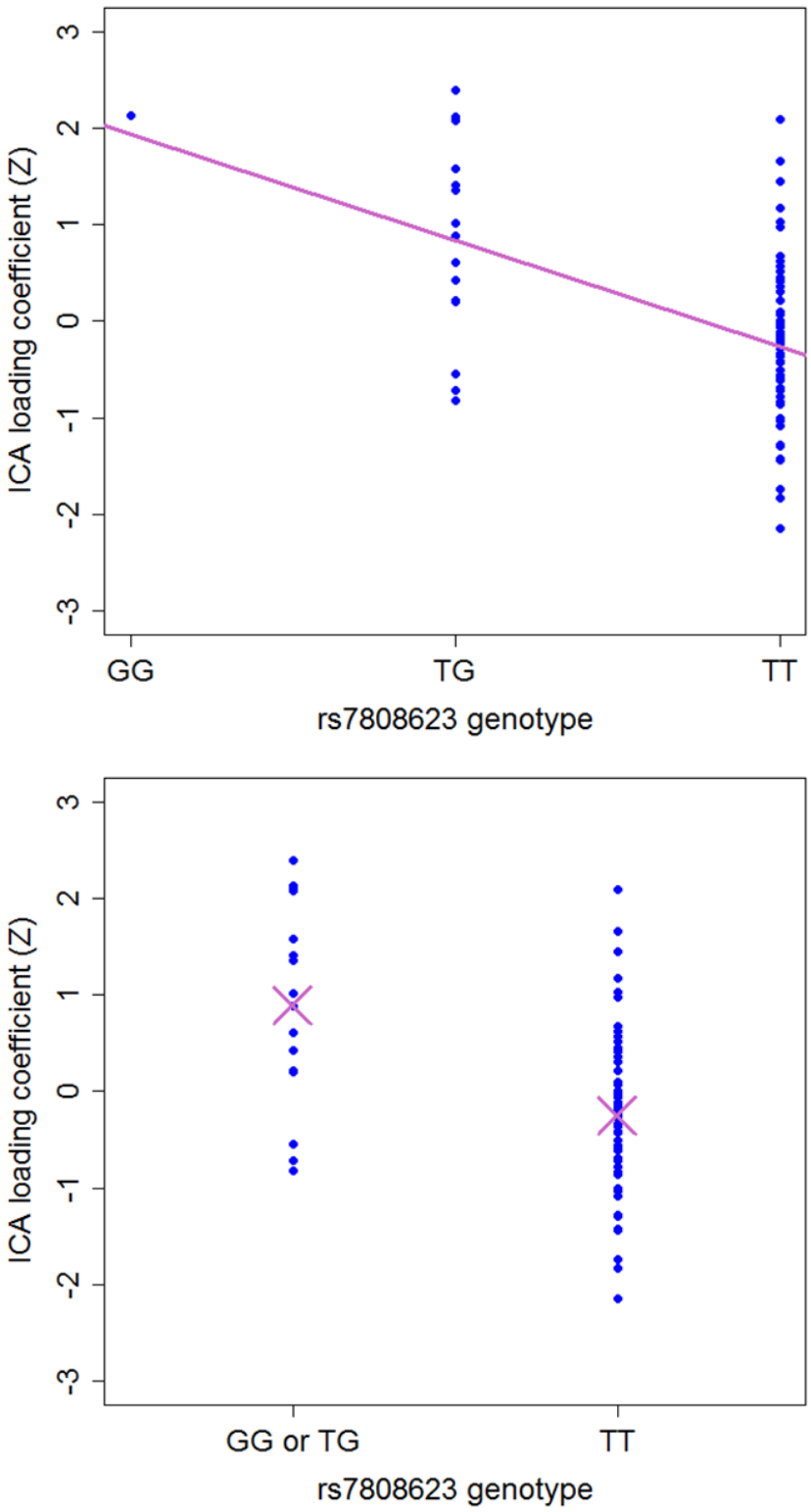

Figure 8: Component B ICA loading coefficients for each subject in the patient group plotted as a function of rs7808623 genotype (A, corrected p with site as a covariate=0.0252) Because there was only one patient subject with a homozygous genotype for the minor allele, that subject was grouped with the heterozygotes to show that the relationship between loading coefficient and genotype still exists (B, corrected p with site as a covariate=0.0542, uncorrected p with site as a covariate=6.75×10^{-5}).

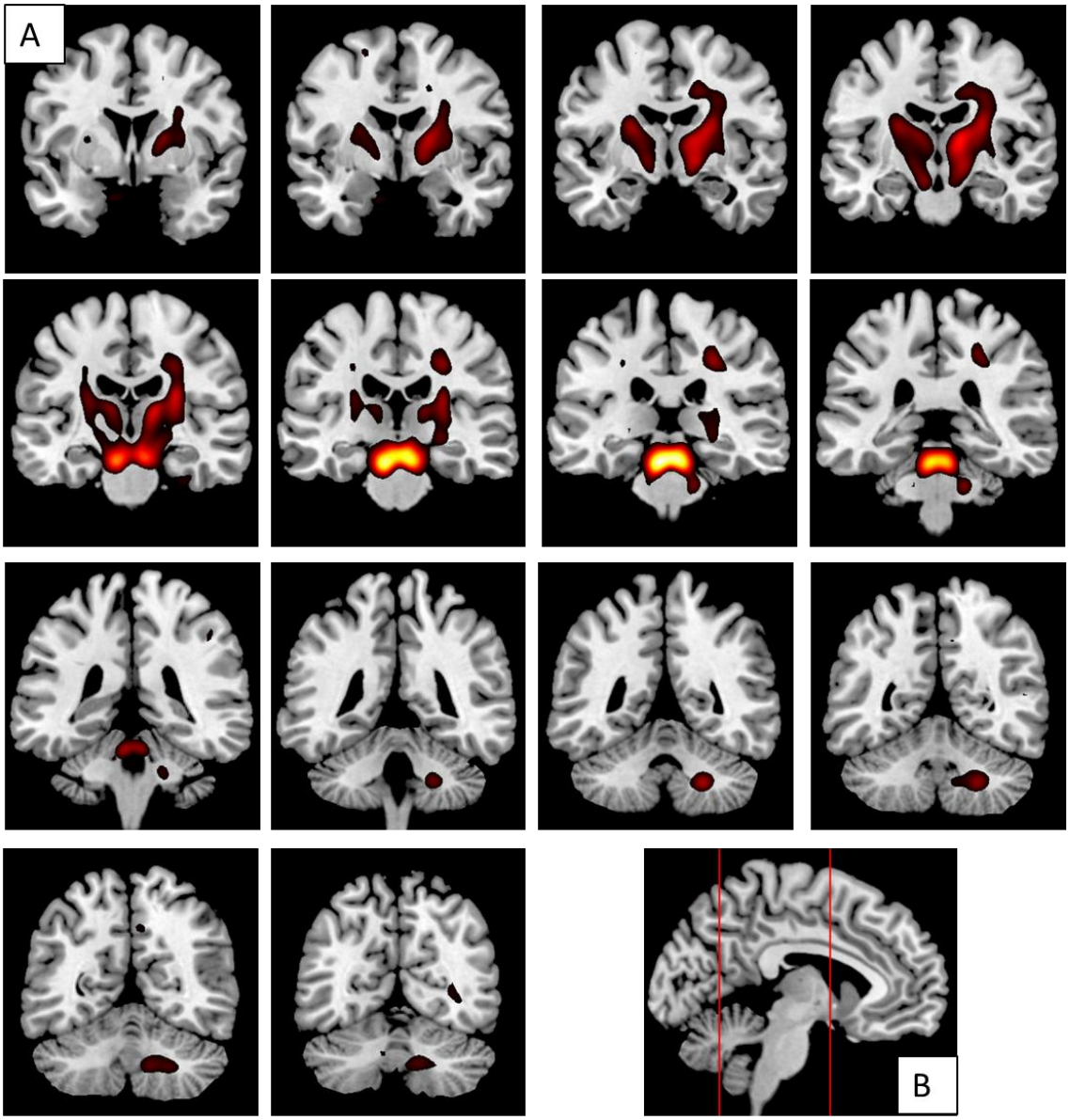

Figure 9: Coronal slices in fixed intervals showing threshold map of component B, starting anteriorly in the top right (A). Sagittal section without threshold map overlay showing interior and posterior boundaries of coronal sections (B)

CHAPTER 4: DISCUSSION

In this study, we obtained both diffusion tensor images and genotypes of 134 myelin and schizophrenia related SNPs in a sample of 74 schizophrenia patients and 87 age- and gender-matched controls. We hypothesized that SNPs in myelin and schizophrenia-related genes would correlate with FA values in biologically relevant independent components obtained from ICA of our DTI data. To our knowledge, this is the first study to use ICA of DTI data to investigate any effect of genotype on FA. We report one SNP, rs7808623, to be significantly associated with white matter integrity in an independent component that contains a large proportion of the cortico-cerebellar-thalamic-cortical circuit (Figure 9) that has long been associated with higher cognitive processes and schizophrenia symptomology (Andreasen et al., 1998).

GRM3

GRM3, also known as metabotropic glutamate receptor 3 (mGluR3), is one of eight metabotropic glutamate receptors (GRM1-8), which are in turn subdivided into three groups based on sequence homology and signaling properties (Nakanishi, 1992; Niswender and Conn, 2010). The metabotropic glutamate receptors appear to be responsible for fine-tuning the actions of ionotropic glutamate receptors (Conn and Pin, 1997; Niswender and Conn, 2010). GRM3, along with GRM2, is a type II metabotropic glutamate receptor and is expressed on the extrasynaptic membranes of presynaptic glutamatergic (Mateo and Porter, 2007) and GABAergic (Mitchell and Silver, 2000) neurons. GRM3 modulates the effects of glutamate spillover by decreasing further

glutamate or GABA release, thereby either decreasing or increasing glutamate-mediated excitation. Binding of GRM3 by glutamate activates $G_{i/o}$ receptors which act to inhibit further neurotransmitter release both by inhibition of adenylyl cyclase and by uncoupling with $G_{\beta\gamma}$ subunits which then directly activate K^+ channels and inhibit Ca^{2+} channels (Niswender and Conn, 2010). Because of its role as an inhibitory receptor on glutamatergic neurons, GRM3 modulates firing of many different kinds of neurons that are innervated by glutamatergic synapses. This includes dopaminergic and serotonergic neurons, both of which are targets of atypical antipsychotics.

Rs7808623 is located in an intronic region of *GRM3* and has not previously been investigated for any functional consequence or association with schizophrenia or white matter. To our knowledge no other studies looking at *GRM3* polymorphisms and schizophrenia have investigated the rs7808623 genotype in particular. Our report that rs7808623 is associated with FA in schizophrenia subjects could indicate that either this SNP is in linkage disequilibrium with another *GRM3* SNP such as rs1476455, which has been shown to be associated with schizophrenia symptom severity (Bishop et al, 2011, see Table 3), or that rs7808623 itself has functional consequences. Intronic SNPs are likely important in *GRM3* expression because *GRM3* is subject to alternative splicing (Sartorius et al., 2006). While our study did not find a difference in any allele frequencies between schizophrenia and control subjects, a positive association between allele frequency and schizophrenia has been shown with at least three other polymorphisms in *GRM3* (Chen et al., 2005; Egan et al., 2004; Fujii et al., 2003; Mössner et al., 2008; Schwab et al., 2008), although other studies have found no association between *GRM3* polymorphisms and schizophrenia (Albalushi et al., 2008; Bishop et al., 2007; Fallin et

al., 2005; Jönsson et al., 2009; Martí et al., 2002; Tochigi et al., 2006). Also, to the best of our knowledge no other study has investigated a relationship between *GRM3* polymorphisms and DTI in either schizophrenia patients or in healthy controls, though other studies have reported a connection between *GRM3* polymorphisms and schizophrenia symptom severity/presentation (Bishop et al., 2011; Egan et al., 2004; Jablensky et al., 2011; Mössner et al., 2008), response to medication (Bishop et al., 2005; Fijal et al., 2009), brain activation patterns (Egan et al., 2004), and brain structure (Haukvik et al., 2010). Table 3 shows the linkage disequilibrium units (LDUs) determined by SNPbrowser between rs7808623 and selected other *GRM3* SNPs reported in the literature as having an association with schizophrenia. LDUs have been proposed to be superior when representing variation of linkage disequilibrium with physical location (Zhang et al., 2002) and for detecting patterns on a small scale (Ke et al., 2004). A linkage disequilibrium block is defined by SNPbrowser as having an LDU value of less than 0.3 (De La Vega et al., 2006). According to this definition, rs1476455 is the only SNP in linkage disequilibrium with rs7808623 in the Caucasian HapMap sample. Linkage disequilibrium in European-Americans has also been reported to extend approximately 60KB (Reich et al., 2001), and both rs2299225 and rs1468412 were reported by SNPbrowser to be within this range (Table 3). Given that these SNPs have been shown to be associated with schizophrenia (Bishop et al., 2011, Chen et al., 2005, Fujii et al, 2003), future studies will need to evaluate of the significance our genetic-neuroimaging findings in a larger cohort of patients and control cases.

SNP	LDUs to rs7808623	Distance to rs7808623	Association with schizophrenia	Reference
rs1476455	0.00 (Caucasian)	61.586 KB	Symptom severity	Bishop et al., 2011
rs2299225	0.32 (Caucasian) 0.17 (Chinese)	42.574 KB	Allele frequency	Chen et al., 2005
rs2237562	0.47 (Caucasian)	67.922 KB	Allele frequency (trend level)	Schwab et al., 2008
rs1468412	0.47 (Caucasian) 1.08 (Japanese)	56.703 KB	Allele frequency	Fujii et al., 2003
rs2228595	0.64 (Caucasian)	74.167 KB	Splice variant	Sartorius et al., 2008
rs6465084	0.64 (Caucasian)	86.679 KB	Allele frequency, global symptom severity, activation patterns during working memory task, attention	Egan et al., 2004; Mössner et al., 2008
rs274622	1.23 (Caucasian)	217.214 KB	Negative symptom improvement with olanzapine treatment	Bishop et al., 2005
rs724226	1.14 (Caucasian)	164.78 KB	PANSS change following risperidone treatment	Fijal et al., 2009
rs2189814	1.14 (Caucasian)	158.398 KB	Cognitive deficit	Jablensky et al., 2011
rs13242038	1.14 (Caucasian)	202.734 KB	Hippocampal volume (not schizophrenia specific)	Haukvik et al., 2010

Table 3: Selected *GRM3* polymorphisms' associations with schizophrenia and distances to rs7808623 in LDUs and MB. Distance was determined using Applied Biosystems' SNPbrowser software. Chinese or Japanese population is also reported if appropriate based on reference's sample population.

GRM3 has been shown to be expressed both in the prefrontal cortex and at lower levels in dopaminergic neurons in the midbrain, although it does not appear to be differentially expressed between schizophrenia patients and controls either in grey matter or in white matter in the PFC (Ghose et al., 2008). Interestingly, agonists of type II metabotropic glutamate receptors have been shown to be effective antipsychotics. In a stage II clinical trial, an agonist of GRM3/GRM2 was shown to be statistically as

effective as olanzapine in reducing symptoms of schizophrenia without the weight gain side effect seen with olanzapine use (Patil et al., 2007). These agonists inhibit the large increase in prefrontal cortex glutamate following treatment of mice with phencyclidine (Moghaddam and Adams, 1998), and they inhibit the large increase in dopamine signaling seen following treatment of mice with ketamine (Fell et al., 2011). These findings suggest that GRM3/GRM2 agonists correct the signaling aberrancies that are responsible for the symptoms of schizophrenia. Adding strength to this hypothesis is the finding that both *GRM2* and *GRM3* knockout mice express more high affinity D2 receptors and are hypersensitive to dopamine neurotransmission (Seeman et al., 2009). Although these pharmacological treatments target both GRM2 and GRM3, it has been suggested that GRM3 especially is responsible for the antipsychotic properties based on the fact that GRM3 polymorphisms, but not GRM2 polymorphisms, have been found to be associated with schizophrenia in several studies (Harrison et al., 2008).

Association of *GRM3* and decreased FA can be explained by a number of reasons. Most obviously, FA decreases with decreased myelination by oligodendrocytes. Cultured rodent oligodendrocyte progenitor cells (OPCs), cultured rodent oligodendrocytes (Luyt et al., 2003; Deng et al., 2004), and adult human OPCs (Luyt et al., 2004) all express GRM3, although any functional role in oligodendrocytes development or myelination has not been completely defined (Luyt et al., 2006). In culture, *GRM3* does not appear to be developmentally regulated (Luyt et al., 2006), and more research is needed to determine its functional role on oligodendrocytes. The *GRM3* association that we observed with FA in our patient sample could also be caused by a decreased number of axons in patients with the TT genotype of rs7808623. Unfortunately, the developmental profile of *GRM3*

in the human brain has yet to be determined, though it has been shown that astrocytic *GRM3* expression is necessary to protect neurons from NMDA-induced neurotoxicity (Corti et al., 2007). This implies that reduced functionality of GRM3, which itself could cause hyper-glutamatergic signaling, could also lead to increased neuronal damage as a result of the aberrant signaling seen in schizophrenia.

Component B/ Cortico-cerebellar-thalamic-cortical circuit

The genotype/FA association we observed occurred in an independent component that was dominated by white matter tracts connecting the internal capsule and the thalamus to the cerebellar peduncles (Figure 9). Although the threshold map of this component does not extend into the prefrontal cortex, component B is still very reminiscent of the cortical-subcortical-cerebellar circuit that was proposed by Andreasen et al. (1998) to be responsible for "cognitive dysmetria" in schizophrenia patients. This circuit is now more often referred to as the cortico-cerebellar-thalamic-cortical circuit. Although the cerebellum has been traditionally viewed as performing mainly balance and motor tasks, it has become increasingly clear that the cerebellum is also involved in tasks related to emotion and cognition (Andreasen and Pierson, 2008). Indeed, the cerebellum has been shown to be active independent of its normal motor function during many activities that are impaired in schizophrenia, including facial recognition (Andreasen et al., 1996), cognitive problem solving and task improvement (Kim et al., 1994; Seidler et al., 2002), emotion attribution (Schulte-Rüther et al., 2007), directed attention (Allen et al., 1997), and working memory (Hayter et al., 2007). Additionally, cerebellar lesions can lead to complex symptomology affecting higher cognitive functions (Schmahmann et

al., 2007; Tavano et al., 2007). Therefore, an altered cortico-cerebellar-thalamic-cortical circuit could be a potential source of many of the cognitive defects seen in schizophrenia.

Further evidence for a loss of connectivity between the cortex and the cerebellum in schizophrenia comes from other diffusion tensor imaging studies that have reported decreased FA in the white matter tracts within the cerebellum and of cortical-cerebellar tracts (Kanaan et al., 2009; Liu et al., 2011; Magnotta, 2008; Solowij et al., 2011). Additionally, several studies have reported reduced cerebellar volume in schizophrenia (Greenstein et al., 2011; Keller et al., 2003; Nopoulos et al., 2009; Thomann et al., 2009), and others have reported reduced blood flow during working memory tasks in regions involved in cortical-subcortical-cerebellar connectivity (Bor et al., 2011; Kiehl et al., 2005; Kim et al., 2009; White et al., 2011).

Although the prominence of the ATR in component B is not apparent from its threshold map, it is worth noting that an analysis mapping each voxel in component B to a DTI atlas mapped 48.4% of component B to either the left or right ATR, a tract that has been reported to have reduced white matter integrity in other DTI and schizophrenia studies (Figure 4, McIntosh et al., 2008; Bora et al., 2011). The ATR is located in the medial portion of the anterior limb of the internal capsule, a tract that is also a part of the cortico-cerebellar-thalamic-cortical circuit . The ATR relays information between the mediodorsal nucleus of the thalamus and the prefrontal cortex (Mori et al., 2005), and loss of integrity of the ATR in particular has been suggested as a partial explanation for some symptoms of schizophrenia (Mamah et al., 2010). In addition to DTI studies in schizophrenia patients, loss of anisotropy in the anterior limb of internal capsule has been reported in temporal lobe epilepsy patients who suffer from psychosis (Sundram et al.,

2010). Interestingly, although we found no statistical difference in white matter integrity between our patients and controls in the independent component that strongly correlated with rs7808623 in our patient sample, we did report a strong difference in anisotropy in another component which contained a large proportion of the ATR (component C, Figures 2C, 3C, 4C, and 6).

Negative results

Our study investigated several SNPs that have previously been shown to be risk factors for schizophrenia (Appendix A), but we failed to show any differences in allele frequencies between our case sample and our control sample. Also, polymorphisms in both *NRG1* (McIntosh et al., 2008A; Winterer et al., 2008) and its receptor *ERBB4* (Konrad et al., 2008; Zuliani et al., 2011) have been shown to be associated with white matter integrity, and we found no such association in our sample. Finally, while many studies have reported an association between white matter integrity and symptom severity (de Weijer et al., 2011; Miyata et al., 2011; Shin et al., 2006; Skelly et al., 2008), we found no such association.

Study limitations

Multi-site studies allow for larger sample sizes, but may cause the risk of inter-site variability. We found that both the variances and the means among the four sites varied significantly, and so we included a site correction for all our analyses. However, we lacked the sample size at any individual site to attempt to reproduce our findings in any one site by itself. Also, our methods required us to correct for 804 independent tests

in the genotype-DTI association study, increasing the possibility of a type II error. Finally, although ICA has several advantages over traditional DTI analysis techniques, a traditional region of interest study would be necessary to confirm a relationship between *GRM3* and the cortico-cerebellar-thalamic-cortical circuit.

REFERENCES

Abbott C, Juarez M, White T, Gollub RL, Pearson GD, Bustillo J, Lauriello J, Ho B, Bockholt HJ, Clark VP, Magnotta V, Calhoun, VD. Antipsychotic dose and diminished neural modulation: A multi-site fMRI study. Progress in Neuro-Psychopharmacology and Biological Psychiatry 35 (2011) 473–482.

Albalushi T, Horiuchi Y, Ishiguro H, Koga M, Inada T, Iwata N, Ozaki N, Ujike H, Watanabe Y, Someya T, Arinami T. Replication study and meta-analysis of the genetic association of GRM3 gene polymorphisms with schizophrenia in a large Japanese case-control population. Am J Med Genet B Neuropsychiatr Genet. 2008; 147:392-6.

Allen G, Buxton RB, Wong EC, Courchesne E. Attentional activation of the cerebellum independent of motor involvement. Science. 1997; 275:1940-3.

Andreasen NC. The Scale for the Assessment of Negative Symptoms (SANS). Iowa City, IA: The University of Iowa; 1983.

Andreasen NC. The Scale for the Assessment of Positive Symptoms (SAPS). Iowa City, IA: The University of Iowa; 1984.

Andreasen NC, Flaum M, Arndt S. The Comprehensive Assessment of Symptoms and History (CASH). An instrument for assessing diagnosis and psychopathology. Arch Gen Psychiatry 1992; 49:615–23.

Andreasen NC, O'Leary DS, Arndt S, Cizadlo T, Hurtig R, Rezai K, Watkins GL, Ponto LB, Hichwa RD. Neural substrates of facial recognition. J Neuropsychiatry Clin Neurosci. 1996; 8:139-46.

Andreasen NC, Paradiso S, O'Leary DS."Cognitive dysmetria" as an integrative theory of schizophrenia: a dysfunction in cortical-subcortical-cerebellar circuitry? Schizophr Bull. 1998; 24:203-18.

Andreasen NC, Pierson R. The role of the cerebellum in schizophrenia. Biol Psychiatry. 2008 Jul 15;64(2):81-8. Epub 2008 Apr 8.

Arfanakis K, Cordes D, Haughton VM, Carew JD, Meyerand ME. Independent component analysis applied to diffusion tensor MRI. Magn Reson Med. 2002; 47:354-63.

Aston C, Jiang L, Sokolov BP. Microarray analysis of postmortem temporal cortex from patients with schizophrenia. J. Neurosci. Res. 2004; 77: 858–66.

Barley K, Dracheva S, Byne W. Subcortical oligodendrocyte- and astrocyte-associated gene expression in subjects with schizophrenia, major depression and bipolar disorder. Schizophr Res. 2009; 112:54-64.

Basser PJ, Mattiello J, LeBihan D. MR diffusion tensor spectroscopy and imaging. Biophys J 1994; 66:259-67.

Basser PJ. Inferring microstructural features and the physiological state of tissues from diffusion-weighted images. NMR Biomed. 1995; 8:333-44.

Bates, D. M. 2006. lmer, P-values and all that. https://stat.ethz.ch/pipermail/r-help/2006-May/094765.html

Benes F. Myelination of Cortical-Hippocampal Relays During Late Adolescence. Schizophrenia Bulletin. 1989; 15:585-593

Bishop JR, Ellingrod VL, Moline J, Miller D. Association between the polymorphic GRM3 gene and negative symptom improvement during olanzapine treatment. Schizophr Res. 2005; 77:253-60.

Bishop JR, Wang K, Moline J, Ellingrod VL. Association analysis of the metabotropic glutamate receptor type 3 gene (GRM3) with schizophrenia. Psychiatr Genet. 2007; 17:358.

Bishop JR, Miller DD, Ellingrod VL, Holman T. Association between type-three metabotropic glutamate receptor gene (GRM3) variants and symptom presentation in treatment refractory schizophrenia. Hum Psychopharmacol. 2011; Epub ahead of print

Bor J, Brunelin J, Sappey-Marinier D, Ibarrola D, d'Amato T, Suaud-Chagny MF, Saoud M. Thalamus abnormalities during working memory in schizophrenia. An fMRI study. Schizophr Res. 2011; 125:49-53.

Bora E, Fornito A, Radua J, Walterfang M, Seal M, Wood SJ, Yucel M, Velakoulis D, Pantelis C. Neuroanatomical abnormalities in schizophrenia: A multimodal voxelwise meta-analysis and meta-regression analysis. Schizophr Res. 2011; 127:46-57

Brouwer RM, Mandl RC, Peper JS, van Baal GC, Kahn RS, Boomsma DI, Hulshoff Pol HE. Heritability of DTI and MTR in nine-year-old children. Neuroimage 2010; 53:1085-92

Brown AS. The environment and susceptibility to schizophrenia. Prog Neurobiol. 2011;93:23-58.

Calhoun VD, Adali T, Pearlson GD, Pekar JJ. A method for making group inferences from functional MRI data using independent component analysis. Hum Brain Mapping 2001; 14:140-51.

Chen Q, He G, Chen Q, Wu S, Xu Y, Feng G, Li Y, Wang L, He L. A case-control study of the relationship between the metabotropic glutamate receptor 3 gene and schizophrenia in the Chinese population. Schizophr Res. 2005;73:21-6.

Cherlyn SY, Woon PS, Liu JJ, Ong WY, Tsai GC, Sim K. Genetic association studies of glutamate, GABA and related genes in schizophrenia and bipolar disorder: a decade of advance. Neurosci Biobehav Rev. 2010; 34:958-77.

Conn PJ, Pin JP. Pharmacology and functions of metabotropic glutamate receptors. Annu Rev Pharmacol Toxicol. 1997; 37:205-37.

Corti C, Battaglia G, Molinaro G, Riozzi B, Pittaluga A, Corsi M, Mugnaini M, Nicoletti F, Bruno V. The use of knock-out mice unravels distinct roles for mGlu2 and mGlu3 metabotropic glutamate receptors in mechanisms of neurodegeneration/neuroprotection. J Neurosci. 2007; 27:8297-308.

De La Vega FM, Isaac HI, Scafe CR. A tool for selecting SNPs for association studies based on observed linkage disequilibrium patterns. Pac Symp Biocomput. 2006:487-98.

de Weijer AD, Mandl RC, Diederen KM, Neggers SF, Kahn RS, Hulshoff Pol HE, Sommer IE. Microstructural alterations of the arcuate fasciculus in schizophrenia patients with frequent auditory verbal hallucinations. Schizophr Res. 2011;130:68-77.

Egan MF, Straub RE, Goldberg TE, Yakub I, Callicott JH, Hariri AR, Mattay VS, Bertolino A, Hyde TM, Shannon-Weickert C, Akil M, Crook J, Vakkalanka RK, Balkissoon R, Gibbs RA, Kleinman JE, Weinberger DR. Variation in GRM3 affects cognition, prefrontal glutamate, and risk for schizophrenia. Proc Natl Acad Sci U S A. 2004;101:12604-9.

Erhardt E, Rachakonda S, Bedrick E, Adali T, Calhoun VD. Comparison of multi-subject ICA methods for analysis of fMRI data. Human Brain Mapping 2011; Epub ahead of print.

Fallin MD, Lasseter VK, Avramopoulos D, Nicodemus KK, Wolyniec PS, McGrath JA, Steel G, Nestadt G, Liang KY, Huganir RL, Valle D, Pulver AE. Bipolar I disorder and schizophrenia: a 440-single-nucleotide polymorphism screen of 64 candidate genes among Ashkenazi Jewish case-parent trios. Am J Hum Genet. 2005; 77:918-36.

Fell MJ, McKinzie DL, Monn JA, Svensson KA. Group II metabotropic glutamate receptor agonists and positive allosteric modulators as novel treatments for schizophrenia. Neuropharmacology. 2011. Epub ahead of print.

Fijal BA, Kinon BJ, Kapur S, Stauffer VL, Conley RR, Jamal HH, Kane JM, Witte MM, Houston JP. Candidate-gene association analysis of response to risperidone in African-American and white patients with schizophrenia. Pharmacogenomics J. 2009; 9:311-8.

First M, Spitzer RL, Gibbon M, Williams JB. Structured clinical interview for DSM-IV-TR axis I disorders. Washington, D.C.: American Psychiatric Press, Inc.; 1997.

Fujii Y, Shibata H, Kikuta R, Makino C, Tani A, Hirata N, Shibata A, Ninomiya H, Tashiro N, Fukumaki Y. Positive associations of polymorphisms in the metabotropic glutamate receptor type 3 gene (GRM3) with schizophrenia. Psychiatr Genet. 2003; 13:71-6.

Greenstein D, Lenroot R, Clausen L, Chavez A, Vaituzis AC, Tran L, Gogtay N, Rapoport J. Cerebellar development in childhood onset schizophrenia and non-psychotic siblings. Psychiatry Res. 2011; 193:131-7.

Hakak Y, Walker JR, Li C, Wong WH, Davis KL, Buxbaum JD, Haroutunian V, Fienberg AA. Genome-wide expression analysis reveals dysregulation of myelination-related genes in chronic schizophrenia. Proc Natl Acad Sci U S A. 2001; 98:4746-51.

Haroutunian V, Katsel P, Dracheva S, Stewart DG, Davis KL. Variations in oligodendrocyte-related gene expression across multiple cortical regions: implications for the pathophysiology of schizophrenia. Int J Neuropsychopharmacol. 2007; 10:565-73.

Harrison PJ, Lyon L, Sartorius LJ, Burnet PW, Lane TA. The group II metabotropic glutamate receptor 3 (mGluR3, mGlu3, GRM3): expression, function and involvement in schizophrenia. J Psychopharmacol. 2008; 22:308-22.

Haukvik UK, Saetre P, McNeil T, Bjerkan PS, Andreassen OA, Werge T, Jönsson EG, Agartz I. An exploratory model for G x E interaction on hippocampal volume in schizophrenia; obstetric complications and hypoxia-related genes. Prog Neuropsychopharmacol Biol Psychiatry. 2010; 34:1259-65.

Hayter AL, Langdon DW, Ramnani N. Cerebellar contributions to working memory. Neuroimage. 2007; 36:943-54.

Jablensky A, Morar B, Wiltshire S, Carter K, Dragovic M, Badcock JC, Chandler D, Peters K, Kalaydjieva L. Polymorphisms associated with normal memory variation also affect memory impairment in schizophrenia. Genes Brain Behav. 2011; 10:410-7.

Jönsson EG, Saetre P, Vares M, Andreou D, Larsson K, Timm S, Rasmussen HB, Djurovic S, Melle I, Andreassen OA, Agartz I, Werge T, Hall H, Terenius L. DTNBP1, NRG1, DAOA, DAO and GRM3 polymorphisms and schizophrenia: an association study. Neuropsychobiology. 2009; 59:142-50.

Jungerius BL, Hoogendoorn MLC, Bakker SC, van't Slot R, Bardoel AF, Ophoff RA, Wijmenga C, Kahn RS, Sinke RJ. An association screen of myelin-related genes implicates the chromosome 22q11 *PIK4CA* gene in schizophrenia. Mol Psychiatry. 2008; 13:1060-8.

Kanaan RA, Borgwardt S, McGuire PK, Craig MC, Murphy DG, Picchioni M, Shergill SS, Jones DK, Catani M. Microstructural organization of cerebellar tracts in schizophrenia. Biol Psychiatry. 2009; 66:1067-9.

Kane JM, Leucht S, Carpenter D, Docherty JP. The expert consensus guideline series. Optimizing pharmacologic treatment of psychotic disorders. Introduction: methods, commentary, and summary. J Clin Psychiatry. 2003; 64 Suppl. 12:5-19.

Ke X, Hunt S, Tapper W, Lawrence R, Stavrides G, Ghori J, Whittaker P, Collins A, Morris AP, Bentley D, Cardon LR, Deloukas P. The impact of SNP density on fine-scale patterns of linkage disequilibrium. Hum Mol Genet. 2004;13:577-88.

Keller A, Castellanos FX, Vaituzis AC, Jeffries NO, Giedd JN, Rapoport JL. Progressive loss of cerebellar volume in childhood-onset schizophrenia. Am J Psychiatry. 2003; 160:128-33.

Kiehl KA, Stevens MC, Celone K, Kurtz M, Krystal JH. Abnormal hemodynamics in schizophrenia during an auditory oddball task. Biol Psychiatry. 2005; 57:1029-40.

Kim SG, Uğurbil K, Strick PL. Activation of a cerebellar output nucleus during cognitive processing. Science. 1994; 265:949-51.

Kim DI, Manoach DS, Mathalon DH, Turner JA, Mannell M, Brown GG, Ford JM, Gollub RL, White T, Wible C, Belger A, Bockholt HJ, Clark VP, Lauriello J, O'Leary D, Mueller BA, Lim KO, Andreasen N, Potkin SG, Calhoun VD. Dysregulation of working memory and default-mode networks in schizophrenia using independent component analysis, an fBIRN and MCIC study. Hum Brain Mapp. 2009; 30:3795-811.

Konrad A, Vucurevic G, Musso F, Stoeter P, Dahmen N, Winterer G. ErbB4 genotype predicts left frontotemporal structural connectivity in human brain. Neuropsychopharmacology. 2009; 34:641-50.

Li YO, Yang FG, Nguyen C, Cooper SR, LaHue SC, Vengopal S, Mukherjee P. Independent component analysis of DTI reveals multivariate microstructural correlations of white matter in the human brain. Hum Brain Mapping 2011; Epub ahead of print.

Liu H, Fan G, Xu K, Wang F. Changes in cerebellar functional connectivity and anatomical connectivity in schizophrenia: A combined resting-state functional MRI and diffusion tensor imaging study. J Magn Reson Imaging. 2011; Epub ahead of print.

Luyt K, Varadi A, Molnar E. Functional metabotropic glutamate receptors are expressed in oligodendrocyte progenitor cells. J Neurochem. 2003; 84:1452-64.

Luyt K, Varadi A, Halfpenny CA, Scolding NJ, Molnar E. Metabotropic glutamate receptors are expressed in adult human glial progenitor cells. Biochem Biophys Res Commun. 2004; 319:120-9.

Luyt K, Váradi A, Durant CF, Molnár E. Oligodendroglial metabotropic glutamate receptors are developmentally regulated and involved in the prevention of apoptosis. J Neurochem. 2006; 99:641-56.

Magnotta VA, Adix ML, Caprahan A, Lim K, Gollub R, Andreasen NC. Investigating connectivity between the cerebellum and thalamus in schizophrenia using diffusion tensor tractography: a pilot study. Psychiatry Res. 2008; 163:193-200.

Mamah D, Conturo TE, Harms MP, Akbudak E, Wang L, McMichael AR, Gado MH, Barch DM, Csernansky JG. Anterior thalamic radiation integrity in schizophrenia: a diffusion-tensor imaging study. Psychiatry Res 2010; 183:144-50.

Matute C. Glutamate and ATP signalling in white matter pathology. J Anat. 2011 Jul; 219:53-64.

Martí SB, Cichon S, Propping P, Nöthen M. Metabotropic glutamate receptor 3 (GRM3) gene variation is not associated with schizophrenia or bipolar affective disorder in the German population. Am J Med Genet. 2002; 114:46-50.

McIntosh AM, Moorhead TW, Job D, Lymer GK, Muñoz Maniega S, McKirdy J, Sussmann JE, Baig BJ, Bastin ME, Porteous D, Evans KL, Johnstone EC, Lawrie SM, Hall J. The effects of a neuregulin 1 variant on white matter density and integrity. Mol Psychiatry. 2008A; 13:1054-9.

McIntosh AM, Muñoz Maniega S, Lymer GK, McKirdy J, Hall J, Sussmann JE, Bastin ME, Clayden JD, Johnstone EC, Lawrie SM. White matter tractography in bipolar disorder and schizophrenia. Biol Psychiatry 2008B; 64:1088-92.

Mitchell SJ, Silver RA. Glutamate spillover suppresses inhibition by activating presynaptic mGluRs. Nature. 2000; 404:498-502.

Miyata J, Sasamoto A, Koelkebeck K, Hirao K, Ueda K, Kawada R, Fujimoto S, Tanaka Y, Kubota M, Fukuyama H, Sawamoto N, Takahashi H, Murai T. Abnormal asymmetry of white matter integrity in schizophrenia revealed by voxelwise diffusion tensor imaging. Hum Brain Mapp. 2011; Epub ahead of print.

Moghaddam B, Adams BW. Reversal of phencyclidine effects by a group II metabotropic glutamate receptor agonist in rats. Science. 1998; 281:1349-52.

Mori S, Wakana S, van Zijl PCM, Nagae-Poetscher LM. MRI Atlas of Human White Matter. 2005. Amsterdam: Elsevier.

Mössner R, Schuhmacher A, Schulze-Rauschenbach S, Kühn KU, Rujescu D, Rietschel M, Zobel A, Franke P, Wölwer W, Gaebel W, Häfner H, Wagner M, Maier W. Further evidence for a functional role of the glutamate receptor gene GRM3 in schizophrenia. Eur Neuropsychopharmacol. 2008; 18:768-72.

Nakanishi S. Molecular diversity of glutamate receptors and implications for brain function. Science 1992; 258:597-603.

Niswender CM, Conn PJ. Metabotropic glutamate receptors: physiology, pharmacology, and disease. Annu Rev Pharmacol Toxicol. 2010; 50:295-322.

Nopoulos PC, Ceilley JW, Gailis EA, Andreasen NC. An MRI study of cerebellar vermis morphology in patients with schizophrenia: evidence in support of the cognitive dysmetria concept. Biol Psychiatry. 1999; 46:703-11.

O'Connell G, Lawrie SM, McIntosh AM, Hall J. Schizophrenia risk genes: Implications for future drug development and discovery. Biochem Pharmacol. 2011;81:1367-73.

Patil ST, Zhang L, Martenyi F, Lowe SL, Jackson KA, Andreev BV, Avedisova AS, Bardenstein LM, Gurovich IY, Morozova MA, Mosolov SN, Neznanov NG, Reznik AM, Smulevich AB, Tochilov VA, Johnson BG, Monn JA, Schoepp DD. Activation of mGlu2/3 receptors as a new approach to treat schizophrenia: a randomized Phase 2 clinical trial. Nat Med. 2007; 13:1102-7.

Reich DE, Cargill M, Bolk S, Ireland J, Sabeti PC, Richter DJ, Lavery T, Kouyoumjian R, Farhadian SF, Ward R, Lander ES. Linkage disequilibrium in the human genome. Nature. 2001;411:199-204.

Rotarska-Jagiela A, Oertel-Knoechel V, DeMartino F, van de Ven V, Formisano E, Roebroeck A, Rami A, Schoenmeyer R, Haenschel C, Hendler T, Maurer K, Vogeley K, Linden DE. Anatomical brain connectivity and positive symptoms of schizophrenia: a diffusion tensor imaging study. Psychiatry Res 2009; 174:9-16.

Sartorius LJ, Nagappan G, Lipska BK, Lu B, Sei Y, Ren-Patterson R, Li Z, Weinberger DR, Harrison PJ. Alternative splicing of human metabotropic glutamate receptor 3. J Neurochem. 2006; 96:1139-48.

Schmahmann JD, Weilburg JB, Sherman JC. The neuropsychiatry of the cerebellum - insights from the clinic. Cerebellum. 2007;6:254-67.

Schulte-Rüther M, Markowitsch HJ, Fink GR, Piefke M. Mirror neuron and theory of mind mechanisms involved in face-to-face interactions: a functional magnetic resonance imaging approach to empathy. J Cogn Neurosci. 2007; 19:1354-72.

Schwab SG, Plummer C, Albus M, Borrmann-Hassenbach M, Lerer B, Trixler M, Maier W, Wildenauer DB. DNA sequence variants in the metabotropic glutamate receptor 3 and risk to schizophrenia: an association study. Psychiatr Genet. 2008; 18:25-30.

Seeman P, Battaglia G, Corti C, Corsi M, Bruno V. Glutamate receptor mGlu2 and mGlu3 knockout striata are dopamine supersensitive, with elevated D2(High) receptors and marked supersensitivity to the dopamine agonist (+)PHNO. Synapse. 2009; 63:247-51.

Seidler RD, Purushotham A, Kim SG, Uğurbil K, Willingham D, Ashe J. Cerebellum activation associated with performance change but not motor learning. Science. 2002; 296:2043-6.

Shin YW, Kwon JS, Ha TH, Park HJ, Kim DJ, Hong SB, Moon WJ, Lee JM, Kim IY, Kim SI, Chung EC. Increased water diffusivity in the frontal and temporal cortices of schizophrenic patients. Neuroimage. 2006; 30:1285-91.

Skelly LR, Calhoun V, Meda SA, Kim J, Mathalon DH, Pearlson GD. Diffusion tensor imaging in schizophrenia: relationship to symptoms. Schizophr Res. 2008; 98:157-62.

Solowij N, Yücel M, Respondek C, Whittle S, Lindsay E, Pantelis C, Lubman DI. Cerebellar white-matter changes in cannabis users with and without schizophrenia. Psychol Med. 2011; 41:2349-59.

Sundram F, Cannon M, Doherty CP, Barker GJ, Fitzsimons M, Delanty N, Cotter D. Neuroanatomical correlates of psychosis in temporal lobe epilepsy: voxel-based morphometry study. Br J Psychiatry 2010; 197:482-92.

Tavano A, Grasso R, Gagliardi C, Triulzi F, Bresolin N, Fabbro F, Borgatti R. Disorders of cognitive and affective development in cerebellar malformations. Brain. 2007; 130:2646-60.

Thomann PA, Roebel M, Dos Santos V, Bachmann S, Essig M, Schröder J. Cerebellar substructures and neurological soft signs in first-episode schizophrenia. Psychiatry Res. 2009; 173:83-7.

Tochigi M, Suga M, Ohashi J, Otowa T, Yamasue H, Kasai K, Kato T, Okazaki Y, Kato N, Sasaki T. No association between the metabotropic glutamate receptor type 3 gene (GRM3) and schizophrenia in a Japanese population. Schizophr Res. 2006; 88:260-4.

Tu PC, Hsieh JC, Li CT, Bai YM, Su TP. Cortico-striatal disconnection within the cingulo-opercular network in schizophrenia revealed by intrinsic functional connectivity analysis: A resting fMRI study. Neuroimage. 2011; Epub ahead of print.

Wahl M, Li YO, Ng J, Lahue SC, Cooper SR, Sherr EH, Mukherjee P. Microstructural correlations of white matter tracts in the human brain. Neuroimage. 2010; 51:531-41.

Wakana S, Jiang H, Nagae-Poetscher LM, van Zijl PC, Mori S. Fiber tract-based atlas of human white matter anatomy. Radiology. 2004; 230:77-87.

Wake H, Lee PR, Fields RD. Control of local protein synthesis and initial events in myelination by action potentials. Science. 2011 Sep 16; 333:1647-51.

Walterfang M, Wood SJ, Velakoulis D, Copolov D, Pantelis C. Diseases of white matter and schizophrenia-like psychosis. Aust N Z J Psychiatry. 2005; 39:746-56. Review.

White T, Schmidt M, Kim DI, Calhoun VD. Disrupted functional brain connectivity during verbal working memory in children and adolescents with schizophrenia. Cereb Cortex. 2011; 21:510-8.

Winterer G, Konrad A, Vucurevic G, Musso F, Stoeter P, Dahmen N. Association of 5' end neuregulin-1 (NRG1) gene variation with subcortical medial frontal microstructure in humans. Neuroimage. 2008; 40:712-8.

Xu L, Groth KM, Pearlson G, Schretlen DJ, Calhoun VD. Source-based morphometry: the use of independent component analysis to identify gray matter differences with application to schizophrenia. Hum Brain Mapping 2009; 30:711-24.

Zhang W, Collins A, Maniatis N, Tapper W, Morton NE. Properties of linkage disequilibrium (LD) maps. Proc Natl Acad Sci U S A. 2002;99:17004-7.

Zuliani R, Moorhead TW, Bastin ME, Johnstone EC, Lawrie SM, Brambilla P, O'Donovan MC, Owen MJ, Hall J, McIntosh AM. Genetic variants in the ErbB4 gene are associated with white matter integrity. Psychiatry Res. 2011; 191:133-7.

APPENDIX A: LIST OF SNPs INVESTIGATED

134 SNPs and their corresponding genes that were investigated for relationship with FA in biologically relevent independent components.

SNP	GeneSymbol	Gene name
rs1801133	MTHFR	5,10-methylenetetrahydrofolate reductase (NADPH)
rs6691840	GRIK3	glutamate receptor, ionotropic, kainate 3
rs364482	EIF2B3	eukaryotic translation initiation factor 2B, subunit 3 gamma, 58kDa
rs2661319	RGS4	regulator of G-protein signaling 4
rs6660593	CNTN2	contactin 2 (axonal)
rs4951161	CNTN2	contactin 2 (axonal)
rs1800896	IL10	interleukin 10
rs841865	PLXNA2	plexin A2
rs752016	PLXNA2	plexin A2
rs7520974	CHRM3	cholinergic receptor, muscarinic 3
rs2919129	RTN4	reticulon 4
rs6715980	RTN4	reticulon 4
rs7601625	RTN4	reticulon 4
rs10496037	RTN4	reticulon 4
*rs2920898	RTN4	reticulon 4
rs2421954	C2ORF86	chromosome 2 open reading frame 86
rs2278718	MDH1	malate dehydrogenase 1, NAD (soluble)
rs7560571	MAL	mal, T-cell differentiation protein
rs16944	IL1B	interleukin 1, beta
rs1344706	ZNF804A	zinc finger protein 804A
rs6435659	ERBB4	v-erb-a erythroblastic leukemia viral oncogene homolog 4
rs7588431	ERBB4	v-erb-a erythroblastic leukemia viral oncogene homolog 5
rs7598440	ERBB4	v-erb-a erythroblastic leukemia viral oncogene homolog 6
rs839523	ERBB4	v-erb-a erythroblastic leukemia viral oncogene homolog 7
rs707284	ERBB4	v-erb-a erythroblastic leukemia viral oncogene homolog 8
rs6436310	PAX3	paired box 3
rs2305234	ARPP21	cyclic AMP-regulated phosphoprotein, 21 kD
rs7372209	CTDSPL	CTD (carboxy-terminal domain, RNA polymerase II, polypeptide A) small

		phosphatase-like
rs3772917	GAP43	growth associated protein 43
rs1370807	GAP43	growth associated protein 43
rs1700	FSTL1	follistatin-like 1
rs8177191	TF	transferrin
rs1799852	TF	transferrin
*rs1358024	TF	transferrin
rs1115219	TF	transferrin
rs1477211	CLDN11	claudin 11
rs6794467	CLDN11	claudin 11
rs2070022	FGA	fibrinogen alpha chain
rs2070016	FGA	fibrinogen alpha chain
rs875462	DTNBP1	dystrobrevin binding protein 1
rs6913660	MHC REGION	major histocombatibility complex region
rs6932590	MHC REGION	major histocombatibility complex region
rs29228	MOG	myelin oligodendrocyte glycoprotein
rs2252711	MOG	myelin oligodendrocyte glycoprotein
rs3130375	MHC REGION/ TCF4	Major histocombatibility complex region/ transcription factor 4
rs3131296	NOTCH4	notch homolog 4
rs11759115	MDGA1	MAM domain containing glycosylphosphatidylinositol anchor 1
rs2064430	AHI1	Abelson helper integration site 1
rs1475069	AHI1	Abelson helper integration site 1
rs2758331	SOD2	superoxide dismutase 2, mitochondrial
rs9456869	QKI	quaking homolog, KH domain RNA binding
rs6964705	EGFR	epidermal growth factor receptor
rs6465084	GRM3	glutamate receptor, metabotropic 3
rs7808623	GRM3	glutamate receptor, metabotropic 3
rs1045642	ABCB1	ATP-binding cassette, sub-family B (MDR/TAP), member 1
rs1128503	ABCB1	ATP-binding cassette, sub-family B (MDR/TAP), member 1
rs7341475	RELN	reelin
*rs1196475	PTPRZ1	protein tyrosine phosphatase, receptor-type, Z polypeptide 1
*rs11136442	ARHGEF10	Rho guanine nucleotide exchange factor (GEF) 10
rs4876268	ARHGEF10	Rho guanine nucleotide exchange factor (GEF) 10
rs2270641	SLC18A1	solute carrier family 18 (vesicular monoamine), member 1
rs35753505	NRG1	neuregulin 1

rs4452759	NRG1	neuregulin 1
rs6994992	NGR1	neuregulin 1
rs10503929	NRG1	neuregulin 1
rs3925	FGFR1	fibroblast growth factor receptor 1
rs6996321	FGFR1	fibroblast growth factor receptor 1
rs2272648	NDRG1	N-myc downstream regulated 1
rs1011784	HSA-MIR-23B	homo sapiens microRNA-23-B
rs913767	GSN	gelsolin (amyloidosis, Finnish type)
rs306761	GSN	gelsolin (amyloidosis, Finnish type)
rs306770	GSN	gelsolin (amyloidosis, Finnish type)
rs3793753	PIP5K2A	phosphatidylinositol-4-phosphate 5-kinase type II-alpha
*rs885834	CHAT	choline acetyltransferase
rs762571	PSAP	prosaposin
rs2299939	PTEN	phosphatase and tensin homolog; phosphatase and tensin homolog pseudogene 1
rs2797986	PLCE1	phospholipase C, epsilon 1
rs4917450	PLCE1	phospholipase C, epsilon 1
*rs521674	ADRA2A	adrenergic, alpha-2A-, receptor
rs2429511	ADRA2A	adrenergic, alpha-2A-, receptor
rs2912787	FGFR2	fibroblast growth factor receptor 2
rs2981428	FGFR2	fibroblast growth factor receptor 2
rs1800955	DRD4	dopamine receptor D4
rs6578993	TH	tyrosine hydroxylase
rs1800532	TPH1	tryptophan hydroxylase 1
rs6265	BDNF	brain-derived neurotrophic factor
rs1602565	INTERGENIC	N/A
rs6277	DRD2	dopamine receptor D2
*rs6275	DRD2	dopamine receptor D2
rs1076560	DRD2	dopamine receptor D2
rs2071521	APOC3	apolipoprotein C-III
rs12807809	NRGN	neurogranin (protein kinase C substrate, RC3)
*rs3016384	OPCML	opioid binding protein/cell adhesion molecule-like
rs705708	ERBB3	v-erb-b2 erythroblastic leukemia viral oncogene homolog 3 (avian)
rs4623951	DAO	D-amino-acid oxidase
rs6311	HTR2A	5-hydroxytryptamine (serotonin) receptor 2A
rs1130233	AKT1	v-akt murine thymoma viral oncogene homolog 1
rs3803300	AKT1	v-akt murine thymoma viral oncogene homolog 1

rs3087454	CHRNA7	cholinergic receptor, nicotinic, alpha 7
rs1355920	CHRNA7	cholinergic receptor, nicotinic, alpha 7
*rs2135551	ADAMTSL3	ADAMTS-like 3
rs4784642	GNAO1	guanine nucleotide binding protein (G protein), alpha activating activity polypeptide O
rs1801200	ERBB2	v-erb-b2 erythroblastic leukemia viral oncogene homolog
rs2070106	CNP	2',3'-cyclic nucleotide 3' phosphodiesterase
rs4796751	CNP	2',3'-cyclic nucleotide 3' phosphodiesterase
rs2258689	MAPT	microtubule-associated protein tau
rs734194	NGFR	nerve growth factor receptor (TNFR superfamily, member 16)
rs1860985	PRKCA	protein kinase C, alpha
rs3813065	PIK3C3	phosphoinositide-3-kinase, class 3
rs470826	MBP	myelin basic protein
rs4890875	MBP	myelin basic protein
rs470131	MBP	myelin basic protein
rs509620	MBP	myelin basic protein
rs2282557	MBP	myelin basic protein
rs4890876	MBP	myelin basic protein
rs2301600	MAG	myelin associated glycoprotein
rs3746248	MAG	myelin associated glycoprotein
rs720308	MAG	myelin associated glycoprotein
rs405509	APOE	hypothetical LOC100129500; apolipoprotein E
rs7412	APOE	hypothetical LOC100129500; apolipoprotein E
rs6140671	PLCB1	phospholipase C, beta 1 (phosphoinositide-specific)
rs762178	OLIG2	oligodendrocyte lineage transcription factor 2
*rs1059004	OLIG2	oligodendrocyte lineage transcription factor 2
rs737865	TXNRD2	thioredoxin reductase 2
rs4680	COMT	catechol-O-methyltransferase
rs701427	RTN4R	reticulon 4 receptor
rs1567871	RTN4R	reticulon 4 receptor
rs165862	PIK4CA	phosphatidylinositol 4-kinase, catalytic, alpha
rs165793	PIK4CA	phosphatidylinositol 4-kinase, catalytic, alpha
rs139884	SOX10	SRY (sex determining region Y)-box 10
rs475827	PLP1	proteolipid protein 1
rs471416	PLP1	proteolipid protein 1
*rs6571291	ABCD1	ATP-binding cassette, sub-family D (ALD), member 1
*rs4129148	CSF2RA	colony stimulating factor 2 receptor, alpha, low-affinity (granulocyte-macrophage)

*Allele frequency for genotype at SNP differed significantly by site ($p<0.05$, X^2 test)